2011-01-01

Investigation On Flame Characteristics Of Oxy-Fuel Combustion

Md R. Islam
University of Texas at El Paso, mrislam@miners.utep.edu

INVESTIGATION ON FLAME CHARACTERISTICS OF OXY-FUEL COMBUSTION

MD RAFIQUL ISLAM

Department of Mechanical Engineering

APPROVED:

Ahsan R. Choudhuri, Ph.D., Chair

Norman D. Love, Ph.D.

Chintalapalle V. Ramana, Ph.D.

Benjamin C. Flores, Ph.D.
Acting Dean of the Graduate School

Dedication

This thesis is dedicated to my parents, my wife, my son, and daughter

INVESTIGATION ON FLAME CHARACTERISTICS OF OXY-FUEL COMBUSTION

by

MD RAFIQUL ISLAM, B.S. EE

THESIS

Presented to the Faculty of the Graduate School of

The University of Texas at El Paso

in Partial Fulfillment

of the Requirements

for the Degree of

MASTER OF SCIENCE

Department of Mechanical Engineering

THE UNIVERSITY OF TEXAS AT EL PASO

December 2011

Acknowledgements

First, I would like to thank my supervisor and committee chair Dr. Ahsan Choudhuri for letting me work with him and in his center for Space Exploration Technology Research (cSETR) lab as a graduate research assistant. He always tried to enhance my knowledge in technical and theoretical perspectives. He always suggested that I work hard and try to learn more things to build a successful career. He always helped me to achieve my goals. Because of his continuous support and guidance over the last two years, I am able to complete this program and graduate successfully. I am grateful to him.

Next, I would like to thank Dr. Norman Love, my co-supervisor, for his continuous support and guidance regarding my research work, thesis writing, and presentation making. He always taught me technical and theoretical knowledge, especially about my research. He spent a great deal of time with me showing how to write a paper, how to present in front of people, and how to organize a thesis.

I would also like to thank Mr. Nathaniel Robinson, Associate Director of the center for Space Exploration Technology Research (cSETR), for always keeping us careful regarding safety considerations and for approving and processing my purchase orders within a very short time.

I would like to thank to all my cSETR lab friends, especially Mr. Bidhan Dam and Mr. Vishwanath for giving me continued technical support.

In addition, I would like to thank the Mechanical Engineering Machine Shop people, especially Mr. David Powell and Mr. Angel Lerma for their generous support related to any issues for my experimental setup.

Finally, I would like to thank the U.S. Department of Energy for funding this project under awards DE-FE-0002402.

Abstract

Oxy-fuel combustion is currently being considered by the U.S Department of Energy as a promising technology for efficient carbon capture. This technology could substantially reduce NO_x and CO_2 emissions. In addition, the implementation of oxy-fuel combustion technology in a power generation system could potentially reduce negative environmental impacts of fossil fuel use. It also encourages the use of reliable and domestic energy sources. The U.S. Department of Energy has made efforts to investigate the performance of a CO_2 and H_2O diluted oxy-fuel combustion system in a high-pressure combustor. In an effort to better understand and characterize the fundamental flame characteristics of oxy-fuel combustion, this thesis presents the flame length, stability of CH_4-O_2/CH_4-O_2-CO_2/ CH_4-O_2-CO_2-H_2O flames, global flame radiation measurements, and flame temperature.

Lengths of oxy-fuel flames mainly depend on fuel firing input and are affected, although less, by O_2 concentration in the fuel-oxidizer mixture. In this study, the stability maps of CH_4-O_2 were plotted using six different tubular burner diameters, ranging from 1 to 6 mm. The flame from the 1 mm diameter burner tube tended to extinguish, even at lower mass flow rates due to a quenching effect. For larger burner diameters, 2 to 6 mm, the flames tended to flashback. It was also observed that the stability regime increased with an increase in CO_2 and H_2O concentration in the fuel mixtures. The radiative heat release rates of CH_4-O_2 flames were greater than CH_4-air flames. The radiative heat release rate of CH_4-O_2 flame was almost constant for the lean flames, yielded F value 4.09%, 8.90% by using solar radiometer and Mark IV radiometer, respectively. Once the equivalence ratio reached more fuel rich conditions, the radiative factor increased as the equivalence ratio increased further. The radiative heat release rates also increased as the percentage of CO_2 increased at a constant fuel firing input. The radiative heat release rates of 75%CH_4-25%CO2-O2 and CH_4-O2 flames were almost similar at constant firing input. As the concentration of CO_2 was increased in the oxidizer, the flame temperature decreased.

Table of Contents

List of Tables

List of Figures

Chapter 1: Introduction

Oxy-fuel combustion is a promising post combustion CO_2 capture technique currently being considered by the U.S. Department of Energy's (2007) Innovations for existing plants program to meet the goal of capturing 90 percent CO_2 capture without increasing the cost of electricity more than 35 percent. In Oxy-fuel combustion, fuel burns with oxygen instead of air to create an exhaust stream containing only CO_2 and H_2O for easy sequestration and storage. Global warming has become an important environmental challenge of the present time. The possible ways to mitigate global warming are increasing energy efficiency, using renewable fuels instead of fossil fuels, increasing the quality of the fuel (high H/C ratio), and carbon sequestration . The CO_2 capture is the most promising because it will take very long time to replace fossil fuels with renewable fuels. Presently renewable sources are used to produce electricity in small scale. The CO_2 capture system is divided mainly into three categories: pre-combustion, post combustion, and oxy-fuel combustion (Buhre et al. 2005). The main challenge in each system lies in separating the CO_2 from flue gas due to the presence of nitrogen (N_2) and low concentration of CO_2. The effectiveness of the carbon capture process is reduced because of the presence of trace impurities (sulfur dioxide and nitrogen oxides). The primary products of the oxy-fuel combustion system are CO_2 and H_2O. Therefore, CO_2 can be easily separated by condensing the water from the exhaust stream and can eventually be stored underground for a long time. The additional advantage of this process is the reduction of nitrogen oxides emissions compared to other processes due to the absence of N_2 in the flue gas.

Increased carbon dioxide levels in the atmosphere have been attributed as the primary contributor to increased global warming. Burning of large amount of fossil fuels especially in power plants is the main source of an increased CO_2 level in the atmosphere. In the power generation system, oxy-fuel combustion technology optimizes the negative environmental impact of fossil fuel use. The increase in awareness of greenhouse gas emissions into the atmosphere has renewed the interest in this

technology, with a focus on: 1) The generation of a CO_2 for easier sequestration, and 2) The use of oxy-fuel and CO_2 for the potential to reduce pollutant emissions, in particular NO_x.

Oxy-fuel technology has not been proven yet to operate in full scale, however, has been confined to laboratory and pilot scale studies. The various groups that cover many of the fundamental issues in science and engineering have identified the issues for oxy-fuel combustion which are: heat transfer, gaseous emissions (environmental issues), ash related issues, combustion, ignition, and flame stability (Buhre et al. 2005). The Jupitar Oxygen Corporation developed an oxy-fuel system, which uses an untempered high temperature oxy- fuel flame, which is currently on the market for environmentally sound energy production (Ochs et al. 2009). The equivalent air-flame temperature is achieved by the addition of recycled CO_2 and H_2O gases into the feed stream. For both turbine cycles and pulverized coal fired plants, several combustor operability issues such as heat transfer characteristics and heat loading, flame stability, and flashback become important with the transition from air to oxygen based combustion (Anderson et al. 2008). Additional O_2 requirements can generate localized O_2 enrichment in the combustor flow-field and disrupt the overall combustor equivalence ratio. The shift in local and global combustor equivalence ratio affects the flame temperature, local burning velocities, and heat release rate, which ultimately lead to a change in combustor transient dynamics in terms of stability, flashback, and heat loading (Anderson et al. 2007 and Ditaranto et al. 2008). Additionally, the introduction of recycled CO_2 and H_2O gases in to the feed stream can change the burner stability.

However, those previous studies on the oxy-fuel flames were conducted under limited conditions. To be used effectively and meet sequestration goals, the fundamental flame characteristics relevant to oxy-fuel combustion are needed to develop new designs and analyze retrofits on existing power generation plants. Therefore, this thesis contributes to current understanding of oxy-fuel combustion through the study of the fundamental flame characteristics and combustor operability issues of oxy-fuel combustion.

1.1 Research objectives

Fundamental flame characteristics data and related burner operability parameters are essential for designing and developing of an oxy-fuel combustion system for new power plants and for retrofitting existing power generation units. Therefore, the objective of this research is to:

1) Develop a series of test matrices to study the stability map of oxy-fuel flame and the effect of CO_2 and H_2O diluents on the stability map;
2) Determine the stability map of oxy-fuel flame using different diameters of burner tube;
3) Understand the effect of diluents, such as CO_2 and H_2O on the stability map;
4) Visualize the CH_4-O_2 ,CH_4-O_2-CO_2 and the CH_4-O_2-H_2O flame at different equivalence ratios;
5) Measure the global flame radiation measurements;
6) Measure and compare the flame temperature of CH_4-O_2 and CH_4-O_2-CO_2 flame.

1.2 Thesis organization

Chapter 1 provides an outline of oxy-fuel combustion and presents the objectives and task associated with this thesis. Chapter 2 provides a summary of the technical background and literature review on the previous worked performed in this field. Chapter 3 provides an outline of the detailed experimental setup and methodology used to determine the stability maps and the fundamental flame characteristics using different burner diameter tubes. The instrument used to carry out the research includes a tubular burner. Chapter 4 presents the comparison, explanation, and discussion of the experimental results for flame stability and some fundamental flame characteristics of oxy-fuels. Chapter 5 concludes the work and provides the scope for further research.

1.3 Practical Relevance

The oxy-fuel combustion technology could substantially reduce NO_x and CO_2 emissions. In addition, the implementation of oxy-fuel combustion technology in a power generation system could potentially reduce negative environmental impact on fossil fuel use. In an effort to develop efficient oxy-fuel burner technologies, flame stability and flame radiation data are required. For this reason, experiments should be focused to generate fundamental flame property data, which include flame shape, radiative heat release factor, flashback, blowout, and flame extinction limits of CH_4/O_2 and H_2-CO/O_2 combustion. The oxy-fuel combustion significantly reduces NO_x emissions due to the absence of N_2 in the oxidizer. The resulting enhanced radiant heat transfer increases combustor efficiency, which results in boiler fuel savings. Reduced fuel consumption results in lower carbon generation, reduced capture costs. Generation of the necessary technical data required to demonstrate the technologies are viable for technical and economic perspective and meet to DOE's Carbon Sequestration Program goals. The outcome of the research will not only improve the fundamental understanding of oxy-fuel combustion but will also provide critical experimental data for the validation of modeling tools. Computational Fluid Dynamics (CFD) analyses are important tools for developing new oxy-fuel burner designs and for analyzing and recommending performance improvements for retrofits. Fundamental flame property data are not currently available in literature to validate CFD analysis models. The outcomes of the proposed research will, therefore, be critically important to meet the validation needs.

1.4 Center for Space Exploration Technology Research (cSETR) Laboratory

The cSETR is located in Mechanical and Industrial Engineering Department at The University of Texas at El Paso. The four laboratories provide 11,000- ft^2 space which allows cSETR to maintain a multitude of diagnostic, experimental and data acquisition capabilities. The infrastructure and equipment

that empowers these capacities include: burner system, vacuum chambers, combustion chambers, projectile proof bunker and remote control room, altitude simulation system, rigs and engines, diagnostic equipment. The primary focus of this research is in the development of micro-propulsion and micro-combustion technologies. The laboratory has state of the art burner and combustion systems, which include a flat flame, nozzle, twin flame counter flow, a tubular burner and swirl stabilized burners. The burner systems are modular and can be changed for various experimental configurations based on research parameters. The burner systems are fitted with pressure sensors, heat flux sensors, a fast thermocouple and digital mass flow controllers and data acquisition systems. The laboratory also has sophisticated flow excitation systems (signal processor, USB audio interface, amplifier, speakers, and probe microphones) required for combustion instability research. These systems are used to determine the combustion characteristics (i.e. flame speed, flashback propensity and flame extinction limits). Apart from this system, the laboratory also provides a collection of optical instrumentation which includes; high-speed camera, intensified CCD camera, laser based measurements techniques, (such as Particle Image Velocimetry (PIV)), as well as a vacuum chamber to replicate the space atmosphere. These systems together comprise the necessary equipment for propulsion systems development. Current fluid dynamics instrumentation in cSETR includes a Laser Doppler Velocimeter (LDV), a multi-channel hotwire (thermal) anemometry system, thermal imaging systems, intensified high-speed camera, various flow controllers, flow meters, and high speed data acquisition systems.

Chapter 2: Background

2.1 Stability

Two types of stability criteria are found in laminar flames. The first type of stability criteria is associated with the ability of the combustible fuel-oxidizer mixture to support flame propagation and is strongly related to the chemical rates in the system. This type of stability limitation includes (1) flammability limit in which gas-phase losses of heat from limit mixtures reduce the temperature, rate of heat release, and the heat feedback, so that the flame is not permitted to propagate and (2) quenching distance in which the loss of heat to a wall and radical quenching at the wall reduce the reaction rate so that it cannot sustain a flame in a confined situation such as propagation in a tube. The second or other type of stability criteria is associated with the mixture flow and its relationship to the laminar flame itself. This type of stability limit, which includes the phenomena of flashback, blow off, and the onset of turbulence.

2.2 Flashback

Flashback occurs in any combustion system at which the flame propagates upstream against the unburned gas (gas stream) into the burner tube. In premixed combustor system, flashback is a critical issue for burner designs. It not only cause serious hardware damages but also increases pollutant emissions. In swirl stabilized lean premixed turbine combustors onset of flashback (Kroner et al, 2003) may occur (i) due to boundary layer flame propagation (critical velocity gradient), (ii) due to turbulent flame propagation in core flow, (iii) induced by combustion instabilities, and (iv) caused by combustion induced vortex breakdown (CIVB).

2.3 Oxy-fuel technology

2.3.1 Industrial

Oxy-fuel combustion is gradually gaining popularity in the industrial production of glasses, aluminum, iron, and steel because of its inherent advantages. These include high combustion efficiency, low volume of exhaust gas, low fuel consumption, high melting capacity, and low NOx emission. The

Jupiter Oxygen Corporation (Ochs Thomas et al. 2009) experimented with a 15 MWth oxy-fuel burner test facility along with Integrated Pollutant Removal (IPRTM) using an untempered high temperature oxy fuel flame, which is unique and environmentally sound among all oxy-fuel systems presently on the market. They observed that all other research groups tried to repeat an air-fuel flame temperature equivalency through the introduction of recycled gas into the oxygen stream to the burner. In addition, the introduction of the primarily carbon dioxide recycled gas into the oxygen stream can cause burner stability problems, making the burner susceptible to flame out. The JOC technology approach has the potential to be extremely stable, and they proved that the untempered high flame temperature oxy-fuel combustion flame can work in a retrofit "D" type boiler. This work was followed up with computer modeling of a 400 MWe boiler. Presently JOC is operating the 15 MWth boilers, where a detailed test program is collecting data on heat transfer with the untempered high temperature flame.

2.3.2 Experimental findings

Lab scale findings

Laboratory scales analyses mainly focus on combustion, heat transfer, and emission characteristics using this technology. Okazaki and Ando (1997) did experiments at an oxygen concentration of 21% and a flame temperature of 1450 K. They identified the separate effects on NO_x emission associated with increased CO_2 concentration, reduction of recycled NO_x, and interaction between fuel-N and recycled NO_x on the decrease of the final NO_x exhausted from the coal combustion system with recycled CO_2. The flame propagation speed of pulverized-coal cloud was measured by Kiga et al. (1997) in a microgravity combustion chamber for determining the ignition characteristic in the CO_2- rich atmosphere. They found that the flame propagation speed in an O_2/CO_2 atmosphere was remarkably low compared with that in O_2/N_2 and O_2/Ar atmospheres at O_2 concentration ranging between 20% and 95%. $CaSO_4$ decomposition was studied on an entrained-flow reactor with model flue gas (O_2:0-30%, CO_2:0-100%) at a temperature of 1400-1600K (Liu H et al. 2000). The results showed

that direct sulfation enables higher degrees of sulfation than those observed from CaO- SO_2 because it is one of the factors to account for its high sulfating efficiency. The sulfation efficiency in conventional coal combustion is usually low due to bonded metal particles; whereas in O_2/CO_2, the decomposition is inhibited and the limestone is subject to a direct sulfation reaction : $CaCO_3 + SO_2 + 1/2\ O_2 \rightarrow CaSO_4 + CO_2$. The emission of CO_2, NO_x, and SO_2 from the combustion of pulverized coal with high oxygen concentration gases were investigated by Hu et al. (2000, 2001, and 2002) in an electrically heated up flow tube furnace at elevated gas temperature 1123-1573 K and the fuel equivalence ratio Φ was varied in the range of 0.4-1.6. They found that NO_x emission indexes decreased monotonically with Φ under both fuel- lean and fuel-rich conditions. CO_2-based inlet gas processes emitted less NO_x than N_2 –based inlet gas processes with same O_2 concentration in inlet gases, whereas SO_2 emissions increased with Φ in fuel lean condition and decreased little more when Φ> 1.2. There was a large effect of temperature on NO_x emission. It was observed that NO_x emission N_2-based inlet gas processes are higher than CO_2-based inlet gas processes (1123 to 1573 K). On the other hand, temperature had little effect on SO_2 emissions.

Pilot scale findings:

As for pilot scale analyses, Kimura et al. (1995) conducted a study with 1.2 MW and Swirl burner. They found that improvement in flame stability and reduction in unburnt carbon content in ash were found with injection of O_2 at the center of the burner. NO_x emission was lower with oxy case but increases with O_2 concentration. SO_x emission was reduced due to condensation of sulfates in ducts and absorption of sulfur in ash. The International Flame Research Foundation in Holland (IFRF, 1995) with 2.5 MW furnace capacity and air-staged swirl-burner did an extensive study. They observed that NO_x emission was greatly reduced with oxy-fuel combustion. Various percentage of the flue gas was recycled and the optimum ratio was found about 0.61. Concentration of CO_2 in the flue gas can be achieved 91.4% or higher with fully optimized conditions. Combustion performance can be achieved

similar to air fired so this technology is suitable for retrofitting. The coal combustion behavior in various mixtures of oxygen and CO_2 were studied by the Canadian CANMET (Croiset and Thambimuthu, 2001) organization with 0.3 MW capacity combustor to demonstrate the effects of several factors on combustion performance. They found that CO_2 concentration in the flue gas achieved close to theoretical value (average 92%). Flame temperature was increased with the increased oxygen concentration at inlet. With 35% oxygen concentration, the flame temperature can be achieved close to air-fired combustion. O_2 purity (<5% N_2) had no significant effect on flame temperature. NO_x emission was reduced in comparison to air-fired case and this reduction can be significant with flue gas recycling. However, if 3% N_2 is present, the difference decreases significantly. SO_2 emission was reduced due to SO_3 formation and sulfur removal. CO emission was decreased with increased oxygen concentration. The Energy and Environmental Research Corporation (EERC) and Argonne National laboratory (ANL), USA (2001) conducted in a pilot scale of 10 million btu/hr boiler capacities for the investigation of flame characteristics. They found that there was a decrease in NO_x (by about 50%) and SO_x emission and the carbon burnout was higher with oxy-coal combustion. No difficulties were found with oxy combustion, so this technology can be applied in full scale. An oxygen concentration of 23.8% (wet recycle) or 27% (dry recycle) was required to match the condition with air combustion. There were no operational difficulties found associated with oxy fuel combustion. A study by Air Liquid together with the Babcock and Wilcox (B & W) company, USA (2004) demonstrated the combustion process with 1.5 MW air staged combustion. They observed that significant reduction in NOx emission with oxy fuel combustion compared to conventional air fired combustion. There was improvement in boiler efficiency due to great reduction in unburnt carbon in fly ash. They reported a significant reduction of Hg emission (around 50%), so suitable flame stability, and heat transfer characteristics could be achieved.

2.4 Combustion characteristics of oxy-fuel flames

2.4.1 Flame stability

For stability perspective, Kim et al. (2006) conducted the flame stability test for various oxy-fuel combustors and they experimentally investigated the NO emission characteristics for the oxy-fuel combustors using flue gas recirculation (FGR). They found that the oxy-fuel combustor with two separate oxidizer nozzles yields the most stable flames in a wide range of CO_2 ratios. As for stability, oxy-fuel combustion with O_2 concentration similar to that found in an air based system cannot be sustained, but requires at least 30% oxygen concentration in the oxidizer stream (Ditaranto and Hals, 2006). Similarly, in pulverized coal units, oxy-fuel systems with flue gas recirculation require an average of 35% concentration in the gas entering into the boiler to maintain the heat transfer characteristics similar to the air fired system (DOE, 2008). LI Guo-neng et al. (2008) carried out an experimental study on the emission characteristics and combustion instabilities of oxy-fuel combustion in a swirl-stabilized combustor. They identified that combustion delay in oxy-fuel combustion was controlled by the oxygen concentration in the oxidant stream, whereas equivalence ratio has a minor contribution to the combustion delay but combustion power has no impact. The combustion instability in oxy-fuel combustions is very different from that in the references cases with similar oxygen concentration. Hjartstam Stefan et al. (2009) with a Chalmers 100 KW test unit conducted the combustion characteristics of lignite-fired oxy-fuel flames in terms of ignition behavior, temperature distribution, and gas composition. The results showed that similar temperature distribution can be achieved in the air and the OF 25 flames at constant stoichiometric ratio condition, whereas in the OF 27 and in the OF 29 case temperatures were higher than in the air case. It is observed that the adjustment of O_2 fraction in the feed gas (i.e. the recycle rate) play an important role, which include gas composition in the furnace, a change in combustion intensity, and important differences in flame stability. However, this does not majorly affect the emission of CO and NO leaving in the furnace. In all oxy-fuel cases

investigated, these emissions are lower than air-fired cases. It was found that appropriate adjustment of the recycle rate is an effective measure to achieve desired combustion stability without any significant impact on emission level. Amato A. et al. (2011) experimentally investigated the flame stability of $CH_4/O_2/CO_2$ flame. They found that operating the CO_2 diluted system significantly contracts operability boundaries due to slower kinetics of this system relative to air. Data and predictions show that the CO_2 diluted system will blow off at flame temperature about 300 K hotter than the air system at a given nozzle exit velocity.

2.4.2 Flame structure

As for flame structure analyses, Kim et al. (2006) had experimentally investigated emission characteristics of the 0.03 MW oxy-fuel combustor under a wide operating range of velocities. They found that the flame length decreased as the fuel or the oxidized velocity increased because of the increased turbulent intensity. In the case of a relatively low fuel velocity ($U_f < 40$ m/s), the flame length substantially decreases with an increasing oxidizer velocity. However, in the case of very high velocity($U_f > 80$ m/s), the flame length slightly decreases with an increasing oxidizer velocity up to 40m/s. Kim Ho Keun and Kim Yongmo (2007) had experimentally investigated combustion characteristics of the air-fuel and oxy-fuel flames in terms of flame length and structure.

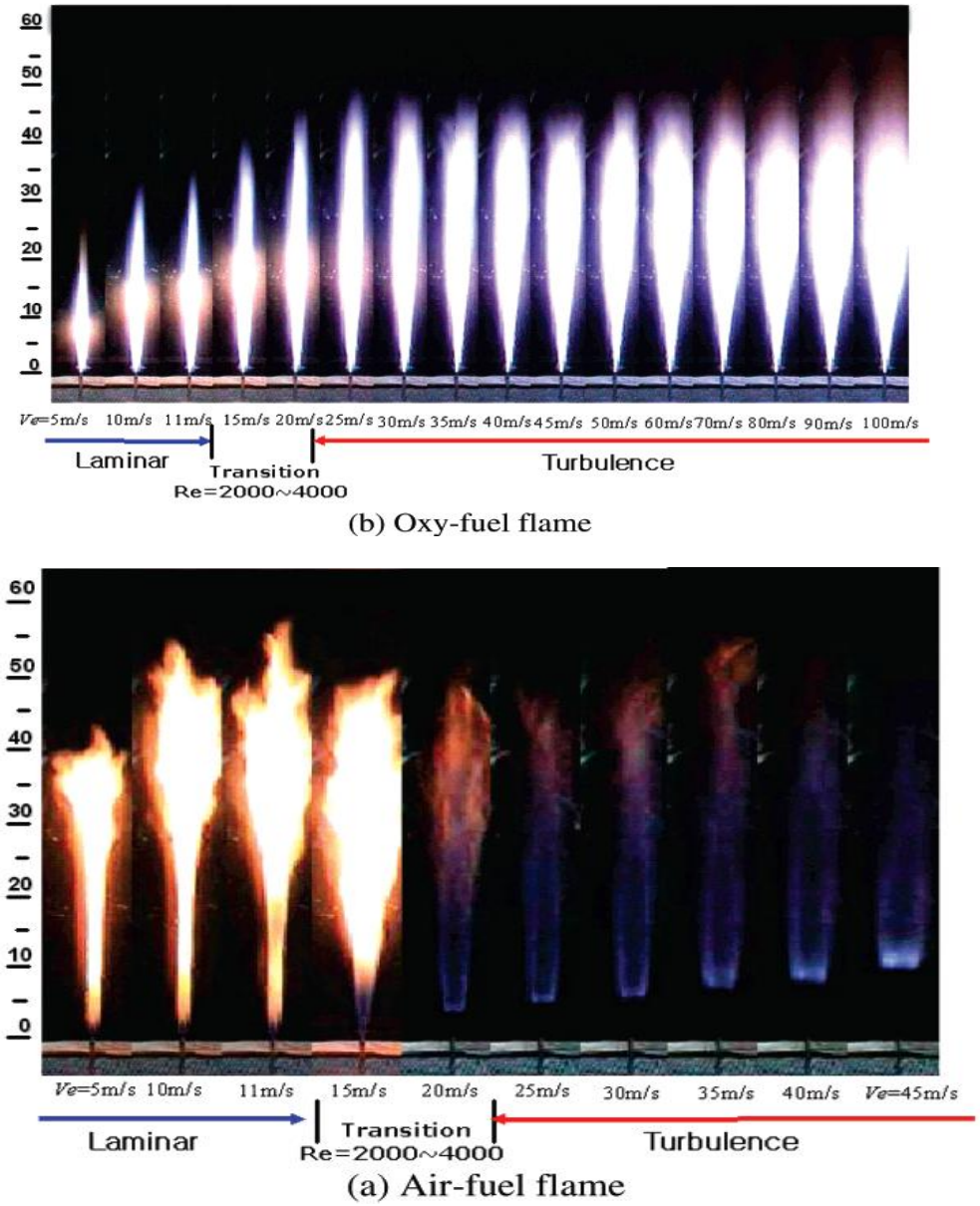

Figure 2.1: Flame images versus fuel velocity for air-fuel and oxy-fuel flames, (Kim Ho Keun and Kim Yongmo, 2007)

It was found that the flame length of the oxy-fuel flame in combustor II decreases with increased fuel velocity or oxygen velocity due to greater turbulent mixing and entrainment. They observed that in figure 2.1 flame length of the oxy fuel flame at the same injection velocity is approximately 40% shorter than air-fuel flame in the laminar flame regime and 10% shorter in the turbulent regime with

small nozzle size (d=2.7 mm). Hjartstam at el. (2009) also compared the flame structure of oxy-fuel cases (obtained by changing the flue gas recycle rate) with an air fired reference case in Chalmers 100 KW test unit. The results showed that similar temperature distribution was achieved in the air and the OF 25 flames at constant stoichiometric ratio condition, whereas in the OF 27 and in the OF 29 case temperatures were higher than in the air case. It is possible to establish an oxy-fuel flame with a flame structure that is almost identical to an air fired case.

2.4.3 Flame Radiation

Andersson and Johnsson (2007) carried out flame radiation characteristic and burnout behavior with different recycled feed gas mixture volumetric concentrations of O_2, Oxygen/Fuel (OF) 21 @ 21% O_2 -79 % CO_2 and OF 27 @ 27% O_2-73% CO_2. The flame emissivity for both cases differs from air-fired conditions. The radiation intensity of the OF 27 flame from inflame soot is higher compared to the air-fired flame. Kim et al. (2007) have experimentally investigated NO_x emission characteristics of oxy-fuel combustors varying CO_2 ratio, Flue gas recirculation (FGR) ratio, and oxygen flow-rate ratio. Five different nozzle arrangement and configurations are designed for oxy-fuel combustors to verify the feasibility of FGR technology. In an effort to understand the NO_x emission characteristics, the authors have used 0.03 and 0.2 MW FGR oxy-fuel combustors. The experimental results showed that the NOx emission level is below 30ppm and 150ppm for 0.03 MW and 0.2 MW oxy-fuel combustors, respectively at the 40% FGR ratio. Andersson et al. (2008) have measured the radiative heat transfer in oxy-fuel flames during combustion of lignite in the Chalmers 100 KW test facility-varying flue –gas recycle rate. Radial profiles of gas concentration, temperature, and total radiation intensity were measured in the furnace. The total radiation intensities increases under oxy-fuel conditions compared to air-firing. The flame temperature and thereby the radiation intensity of the flame, increases with decreasing recycle rate or increasing O_2 concentration in the recycled flue-gas. However, the total

intensities become similar for air-fuel and oxy-fuel conditions as long as the gas temperatures are similar because particles contribute a significant fraction of the total radiation emitted by lignite flames.

2.5 Opportunities and challenges

2.5.1 Opportunities

Emission control:

The emission of injurious substances from oxy-fuel system can be made zero or close to zero. CO_2 the primary contributor to global warming, can be captured safely employing this method. Various pilot scale studies showed that the concentration of CO_2 in the flue gas can be achieved on average 92% (Buhre et at. 2005). Separation of CO_2 is easier in oxy-fuel case because the product of combustion is mainly CO_2 and water vapor. By condensing the water vapor, CO_2 can be easily captured, which can be sequestrated in many ways. Since the large volume of N_2 is absent in the flue gas, it is possible to use sulfur removal equipment and NO_x removal equipment smaller in size, which in turn reduces the cost compared to air-fired case. Though some CO_2 may be dissolved in condensed water or may be lost during processing of other non-condensable gases, most of it can be captured. Therefore, from the emission point of view, oxy-fuel technology has huge potential. Several pilot studies showed reduction in NO_x emission and improvement in carbon burnout.

Reduction of heat losses in the boiler:

In oxy-fuel technology, fuel is burned with pure oxygen rather than air in which large volume of N_2 (78%) is present. This inert N_2 carry a significant amount of heat after the combustion. This heat is lost as the exhaust gas is released to the atmosphere since the exhaust gas has higher temperature than atmospheric condition. The heat loss due to N_2 in an air-fired case accounts up to 10% (Jordal et al.,

2004). In oxy-fuel combustion, almost no N_2 is present during combustion. Therefore, this heat loss due to N_2 is reduced significantly.

Optimizing boiler design:

In oxy fuel, the combustion phenomenon is different from conventional air-fired combustion. The large volume of N_2 in air acts as a diluents when fuel is fired with air. Due to the absence of N_2 in oxy case, flame temperature becomes too high. To limit the temperature and make up for missing N_2, a large part of the flue gas is recycled. With development of technology, it is possible to arrange an internal recycling of the flue gas inside the boiler. Internal recycling of flue gas has several advantages as the size of the boiler is reduced significantly, radiation heat loss by the flue glass is reduced, and the power required flue gas recycling is decreased. The reduction in boiler size associated with the reduction in initial investment on the boiler.

2.5.2 Challenges

Though oxy fuel technology was offered in the eighties, still it is limited to laboratory scale and pilot scale studies. This technology involves several technical challenges that warrant further investigation. Significant amount of energy is required by an air separating unit and a CO_2 processing unit, which reduces the efficiency of the oxy coal system. Figure 2.2 shows the efficiency of an oxy-coal system compared to conventional an air-fired plant (Hack and Shah, 2008).

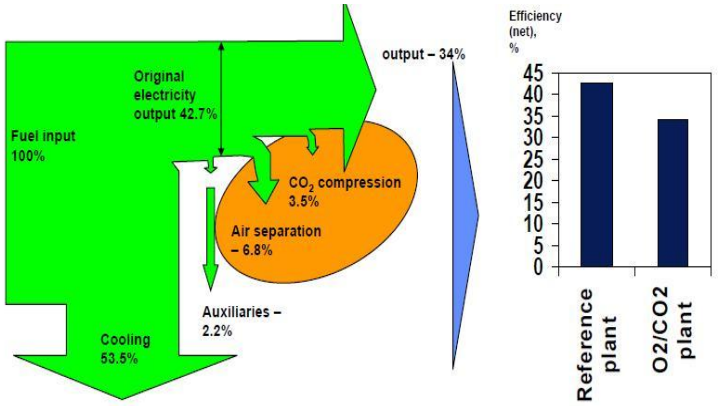

Figure 2.2: Efficiency of an oxy-coal system compared to conventional air-fired plant, (Hack and Shah, 2008).

Boiler design:

The main challenge in oxy-fuel combustion technology is to design a boiler, which will operate in optimized conditions. Since the coal is burnt with pure oxygen, many changes occur. Heat transfer characteristics are changed due to large concentration of CO_2 in the flue gases. Higher flame temperature results from burning with pure oxygen. To reduce the temperature, a large portion of flue gas is recycled. To increase boiler efficiency and to reduce boiler size, external recirculation percentage must be reduced and arranged an internal recycling system inside the boiler to cool the flame. There are challenges involved with designing a boiler with internal recycling system. In external flue gas recycling, the recirculation extraction point is also an important factor to avoid large accumulation of the particulates. The particles should be removed before the recycling point. Addition of oxygen inside the boiler is also an important factor to regulate the NO_x and CO emission. The boiler should be properly sealed to avoid air leakage; if it leaks then there must be provision for separating it from the downstream flue gases. Choosing materials for the boiler is another critical issue. The heat flux to the wall and super heaters is increased due to high CO_2 content in the flue gases; therefore the corrosion condition is more favorable in oxy-fuel combustion compared to conventional air-fired combustion. The formation of SO_3

also leads to an increase in corrosion. By investigation the corrosion behavior, boiler material should be chosen carefully.

Air Separation Unit (ASU):

The air separation unit has a great impact on the efficiency of the oxy-fuel combustion system. The power consumption by this unit is the critical factor. A large commercially available large air separation unit uses the cryogenic distillation principle to separate N_2 and O_2 from the air. The cryogenic process uses thermally linked high-pressure and low pressure distillation columns.

CO_2 processing:

The product of combustion in oxy-fuel cases include mainly CO_2 and water vapor, with small amount of SO_x, NO_x and other non condensable gases like Ar, Air,N_2, and excess O_2. Although it is possible to capture almost all CO_2 from the flue gases, the cost of CO_2 processing has a significant impact on the plant efficiency. Depending on the application, CO_2 purity varies. Besides the preceding factors, cost involvement of particle removal, flue gas condenser, and SO_2 emission control should also be considered.

However, those previous studies on oxy-fuel flames were conducted under limited conditions. The design of the oxy fuel combustor requires detailed information about the oxy-fuel flame structure, as well as a comprehensive research effort that includes sequences of trial-and-error testing, combustion measurements, and analyses, since the stability limit includes the phenomena of flashback, blow off, and onset of turbulence. Therefore, this paper presents the fundamental flame characteristics and combustor operability issues (flash back/blowout) of oxy-fuel combustion.

Chapter 3: Experimental Facilities

3.1 Tubular Burner

To conduct the experiment, a tubular burner was designed to be operated in both lean and rich condition. The burner is designed in such a way that it can withstand the high temperatures of oxy-fuel flame. One of the main criteria of the burner is to investigate flame characteristics with respect to various burner diameters. Finite element analysis was carried out under thermal stress using NASTRAN 6.1 to withstand a high thermal load. The final design of the tubular burner used for the experiments is shown in Figure 3.1.

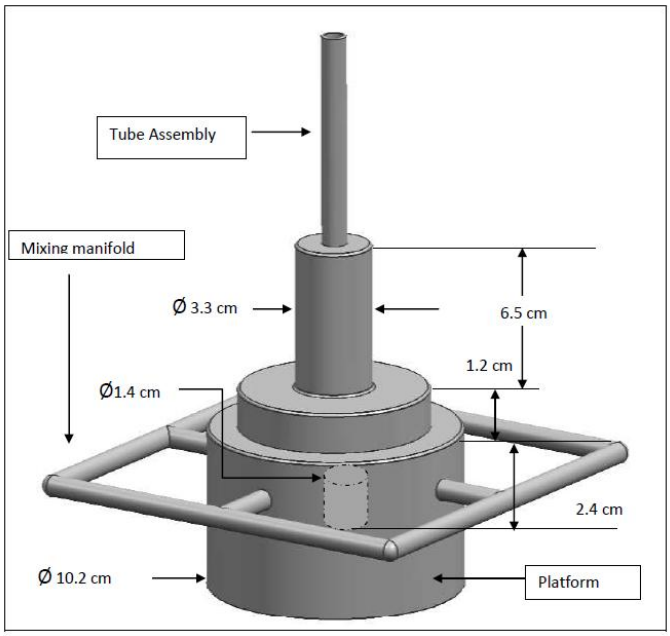

Figure 3.1: Schematic diagram of the tubular burner.

The designed tubular burner system mainly consists of three sections: (a) platform, (b) mixing manifold, and (c) burner tube assembly. Different diameters of tubes are accommodated in the tube assembly

section, which merge with the adapters. In the burner system, there are four alternate injection holes into the manifold. Figure 3.2 shows the using different types of inner diameters of stainless steel tube.

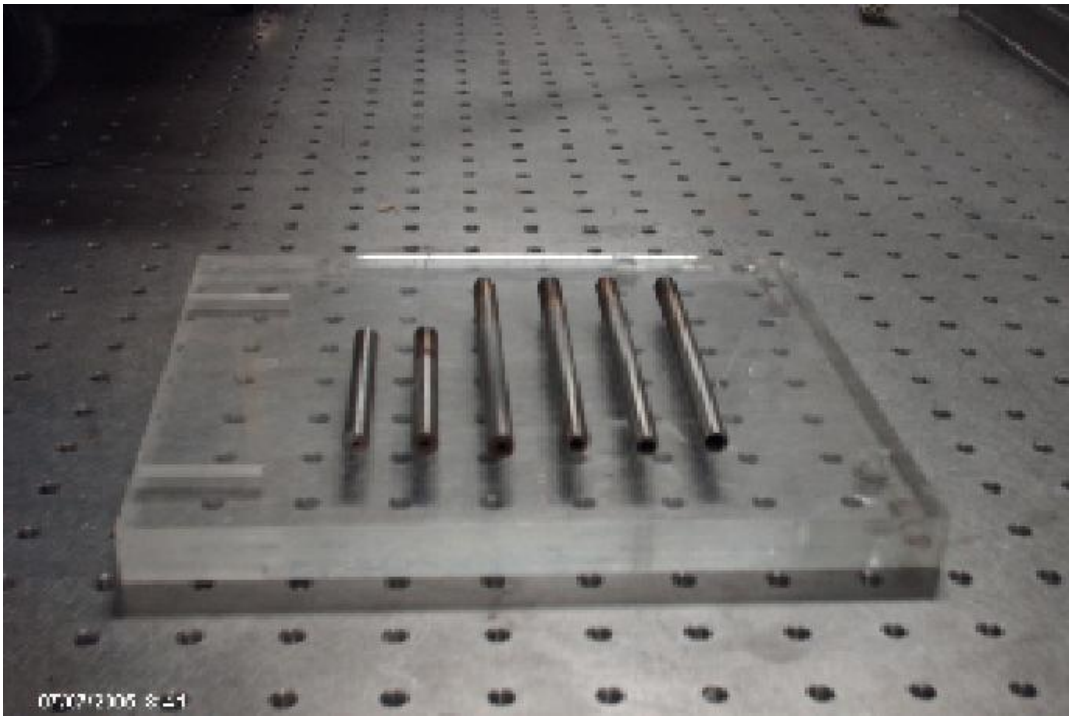

Figure 3.2: Different types of inner diameters (1mm-6 mm) of stainless steel tubes.

3.2 Experimental setup

A schematic diagram and experimental setup for oxy-fuel flame stability, flame length, and flame temperature measurements are depicted in Figure 3.3 and Figure 3.4. Plexiglas is used for shielding the tubular burner and putting the exhaust pipe on the top of the Plexiglas. The Plexiglas is visually inspected for damage or deformation. Premixed fuel and oxidants are injected into the burner manifold through four alternate injection holes from pressurized gas cylinders. The fuel used for this experiment was methane, and the oxidants used were oxygen and carbon dioxide. Digital mass flow meters were used to measure mass flow rates of fuels and oxidant composition. Prior to mixing and delivery to the burner, individual manual precision metering valves were used, in conjunction with low-torque-quarter-turn plug valves, to control the mass flow rate of fuel and oxidant composition. To reduce

errors, prior to each experiment mass flow meters were calibrated, using a laser based mass flow meter calibrator. A flame arrestor device was installed in the line, before the burner manifold, to prevent flashback and for safety. The premixing fuel and oxygen mixture was ignited with an external ignition source. The resulting flame was analyzed with the use of a high-resolution digital SLR camera. Flame stability, flame temperature, and flame length were tested at different firing rates, recirculation ratios, flow rates, and equivalence ratio conditions. Flame stability was investigated on combustor operability issues of flashback and blowout using different diameters of burner. Flame lengths were measured using the end of the visible part of the luminous portion of the flame. Flame temperatures were measured by s-type thermocouple above two-third heights of flame length at equivalence ratio (Φ) =1 condition.

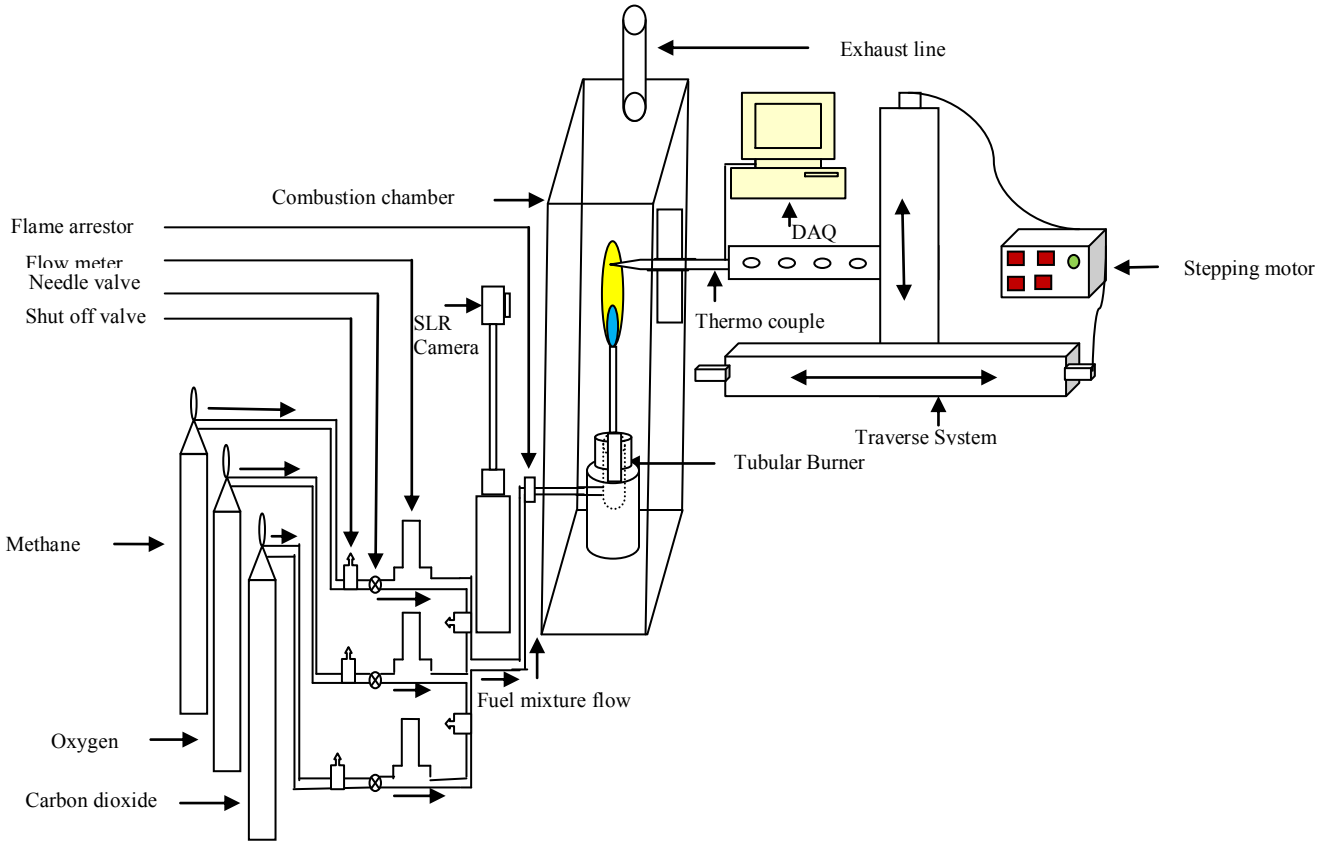

Figure 3.3: Schematic diagram for experimental setup of flame stability, flame length and flame temperature measurements

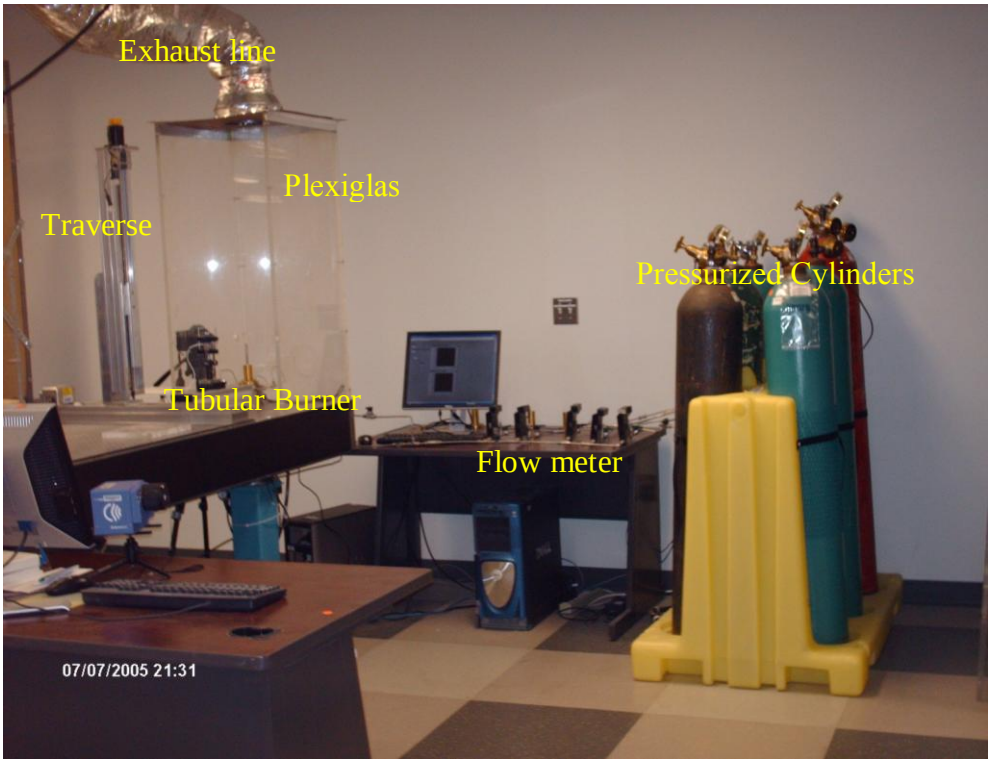

Figure 3.4: Experimental setup for flame stability, flame length, and flame temperature measurements.

A schematic diagram and complete experimental set up for global flame radiation measurements are shown Figure 3.5 and Figure 3.6. For this experiment, two different types of radiometer have been used to measure the flame radiation. A Mark IV series non-contact temperature sensor & radiometer with 150° view angle and 0.1 to 92 µm wavelength ranges is used to measure global flame radiation. Solar flux radiometer is also used, with a view angle of 180°and 0.1 to 20 µm wavelength ranges to measure oxy-fuel flame radiation. During the experiment, the distance between flame and radiometer was considered as a radius of the flame. For these experiments, the radiative heat release factor (F) is calculated using Eq. (1):

$$F = \frac{q_r}{q_{in}} \tag{1}$$

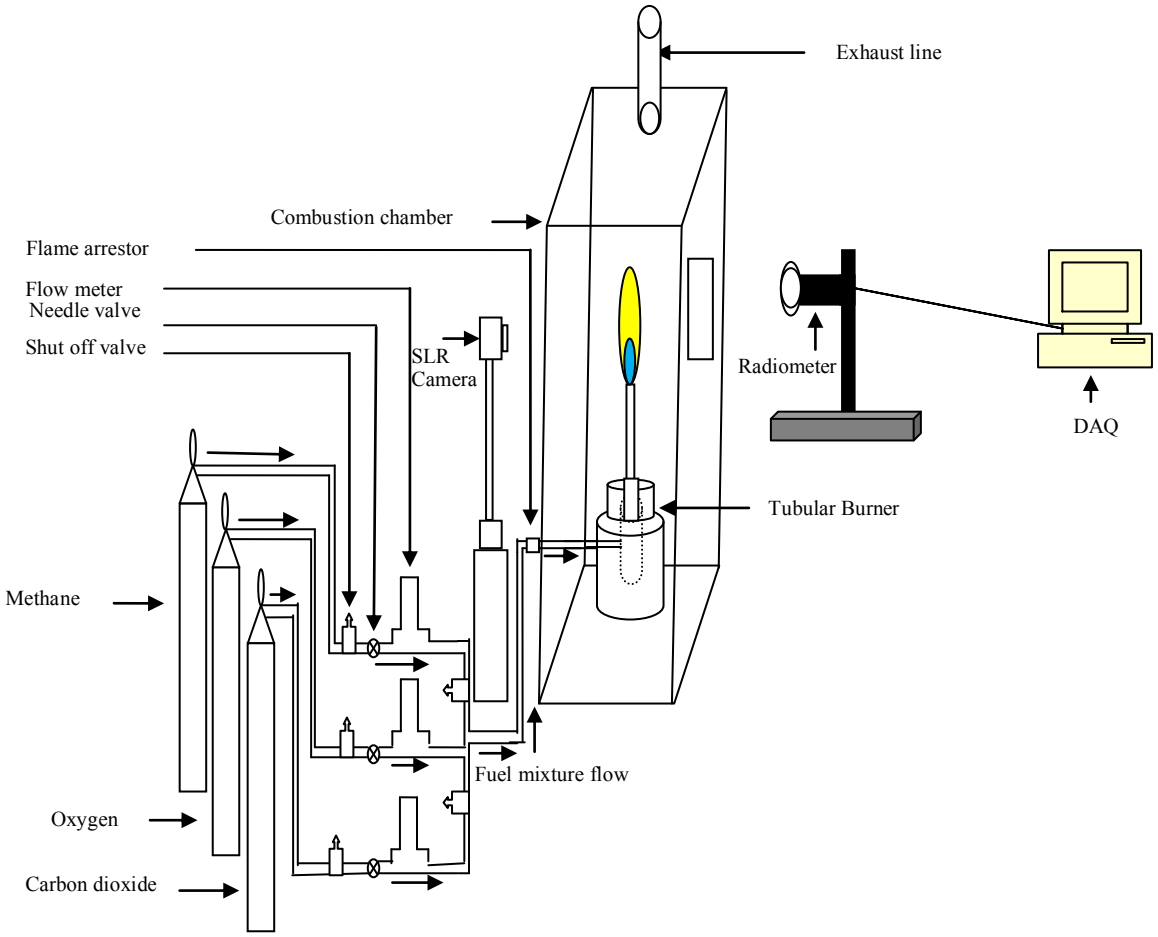

Figure 3.5: Schematic diagram for experimental setup of global flame radiation measurements.

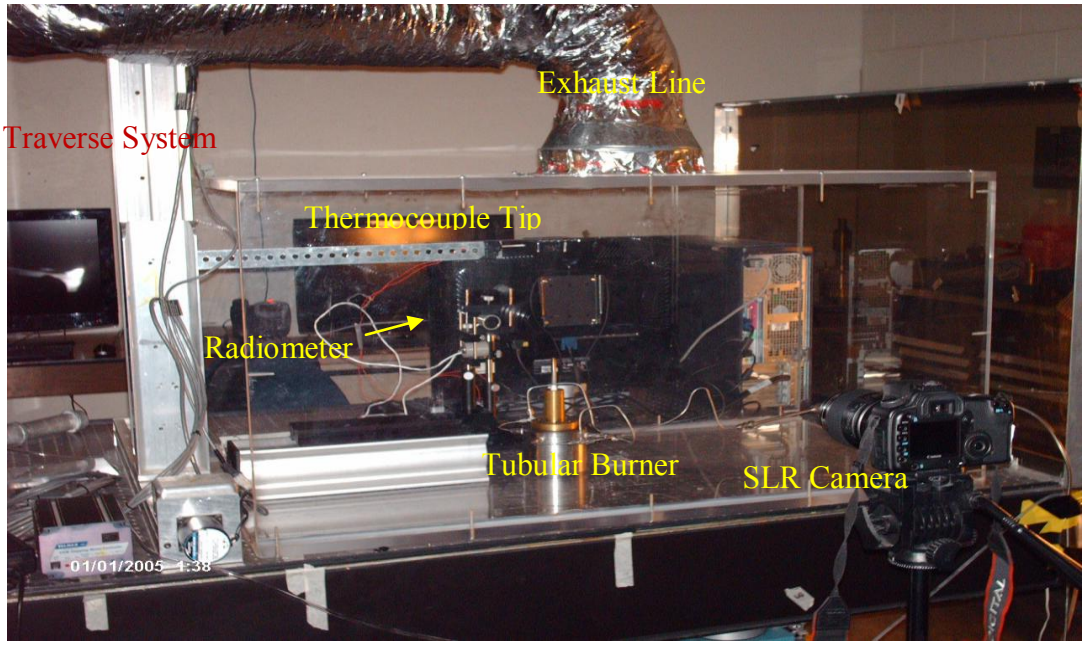

Figure 3.6: Complete experimental setup for global radiation measurements.

Where q_r is the radiation output and q_{in} is the firing input to the combustion. As discussed later, the adiabatic flame temperature was calculated using STANJAN commercial software by disregarding CO_2 and H_2O dissociation at that temperature. Experimental uncertainties were calculated using Student-t distribution with 95% confidence interval. Experimental uncertainties of present measurements are less than ±2% of the mean value.

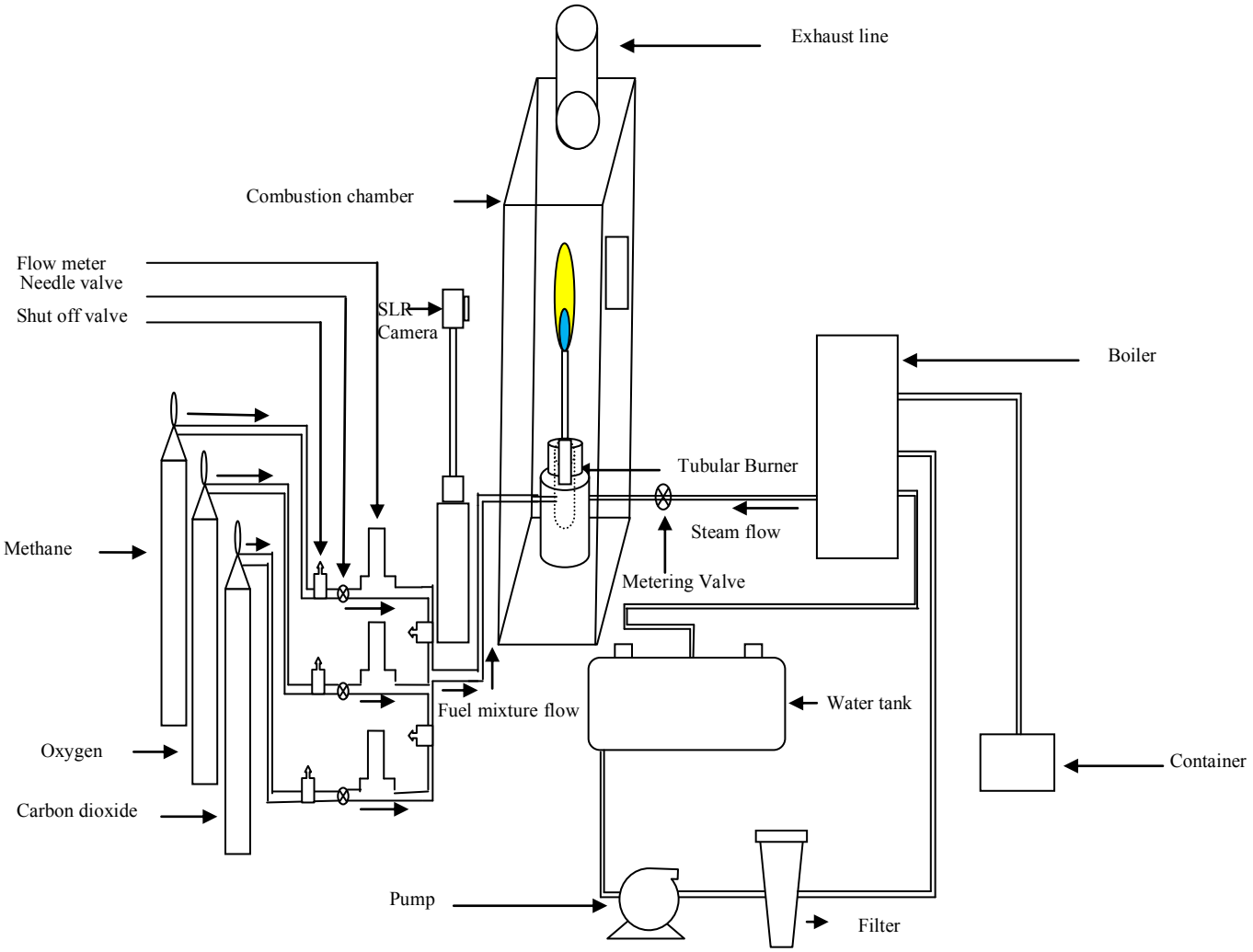

Figure 3.7: Schematic diagram for experimental setup of steam recirculation.

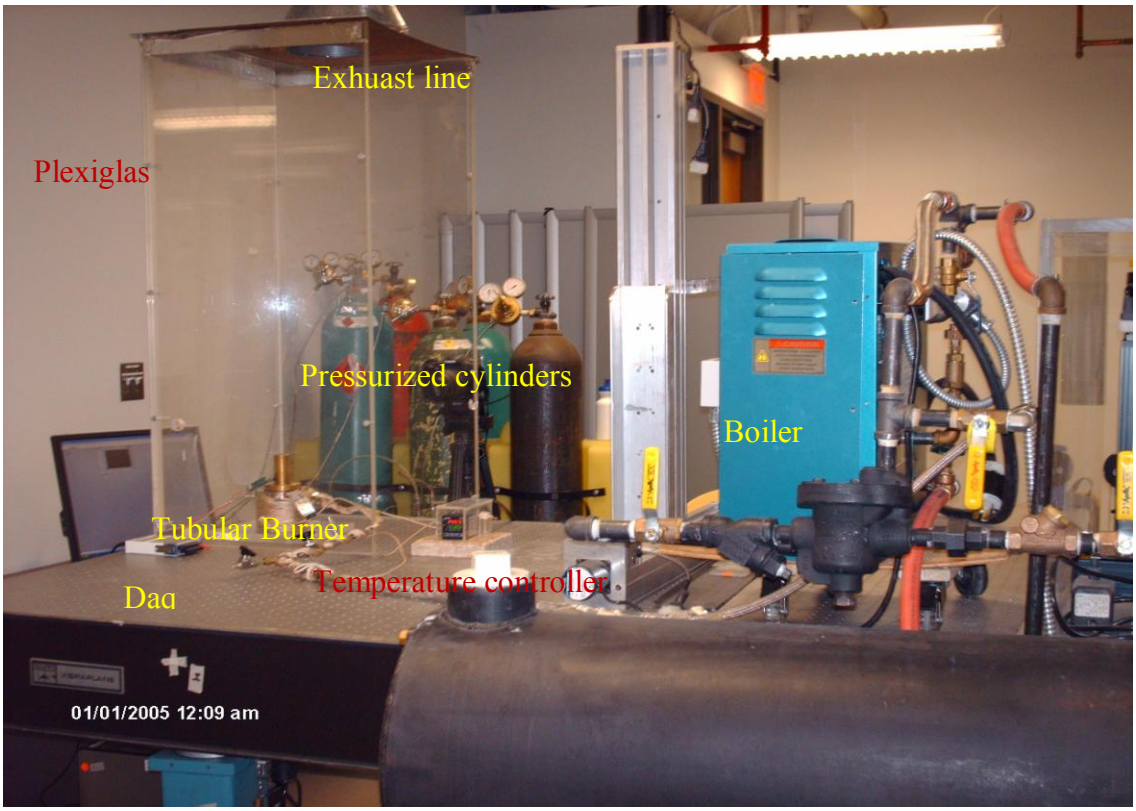

Figure 3.8: Experimental setup for analyzing the effect of steam recirculation.

A schematic diagram and complete experimental setup for analyzing the effect of steam recirculation are shown in Figure 3.7 and Figure 3.8. A laboratory scale Boiler system and its auxiliaries were used for making steam to be recirculated in the burner. For keeping steam throughout the line to the burner, heavy insulated high temperature heater tape was used for keeping continuous heat. Temperature controller CN7800 series was used to control the required temperature in the line and the burner. The combination of these components allows the group to analyze the effect of steam recirculation in the burner

3.3 Boiler System

The products of oxy-fuel combustion are mainly carbon dioxide and steam. For recirculation of steam to the burner, a laboratory scale, MBA Electric Steam Generator (MBA6, 6 KW, 100 PSIG), in

figure 3.9 was used for the generation of steam. The standard features of the Electric Steam Generator are that it automatically maintains proper water level, allows constant observation of water level while the boiler is in operation, integral electrical control, long life heating elements, operating pressure control, steam safety valve, visual observation of steam pressure over full range, and fully insulated pressure vessels, which minimize heat loss and maximize energy savings. The production of steam rate was 18 lbs/hr. The product of steam was recirculated to the burner for the investigation of flame stability.

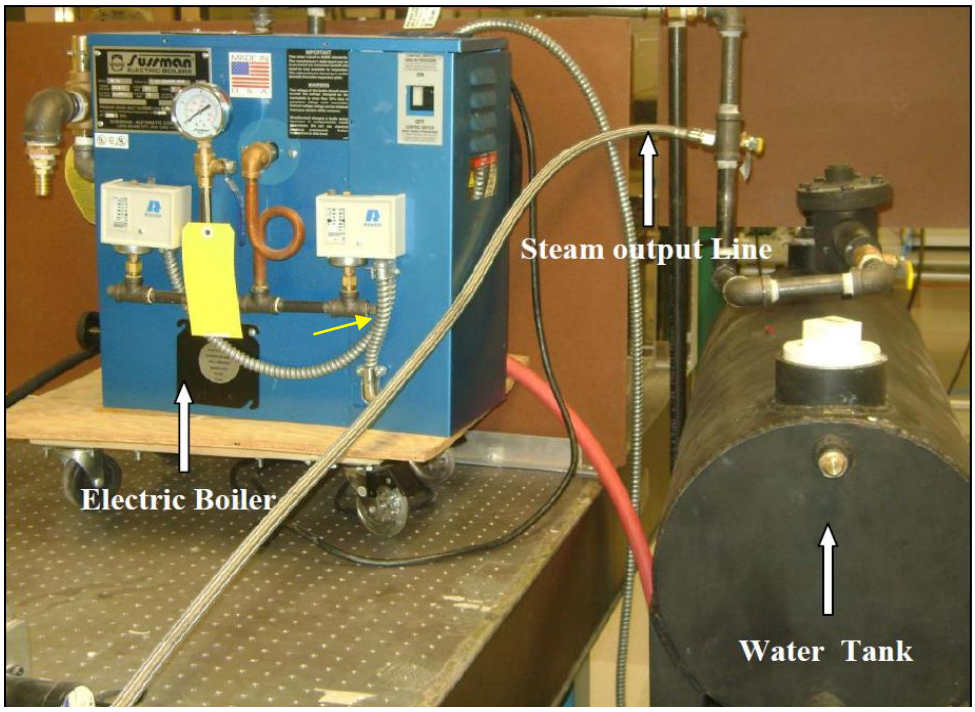

Figure 3.9: Boiler System.

3.4 Flow Measurement Devices and Data Acquisition

3.4.1 Flow meter

Digital mass flow meters (Omega FMA 1700/1800 series in figure 3.10) were used to measure the mass flow rate of fuel and oxidant. The mass flow meters are designed to withstand temperatures ranging from 0^0 C to 50^0 C, pressures up to 500 psig and relative humidity of 70%. The mass flow

meters used in the present study varied in full scale from 0-2L/min, 0-5L/min, and 0-10L/min. For all cases, the accuracy is ±1.5 percentage of the full scale. The mass flow meter is shown in figure 3.10. To reduce error, prior to each experiment, mass flow meters are calibrated by using Dry Cal Meter calibrator as shown in figure 3.11.

Figure 3.10: Digital Mass Flow Meters

Figure 3.11: Dry cal calibrator.

3.4.2 Shutoff and Metering Valves

The shutoff valves (SS-4P4T4 in Figure 3.12) were used to shut off the fuel flow from the pressurized gas cylinders. Manual precision metering valves (SS-SS4VH in Figure 3.13) were used to regulate the O_2 and fuel mixture.

Figure 3.12: Swagelok SS-4P4T4 shutoff valve.

Figure 3.13: Swagelok SS-SS4VH metering valve

3.4.3 Data Acquisition

For temperature measurement, a National Instrument Lab View data acquisition system is constructed to attain signals from the individual sources. The input module is shown in Figure 3.14.

Figure 3.14: NI USB 9263

The NI USB 9263 is a four channel, 16-bit analog voltage output module and ranges from-10 volts to +10 volts. Two S-type thermocouples are connected to the two channels by means of long connecting wires. The s-type thermocouple is generally comprises of platinum and platinum-10% rhodium (Figure 3.15).

Figure 3.15: S-type thermocouple

The USB data acquisition is capable of recording data at 12 samples per second. For this experimental purpose, it is more than sufficient to get the temperature readings. The virtual instrument designed for this purpose is shown in Figure 3.16 and the related block diagram is shown in Figure 3.17.

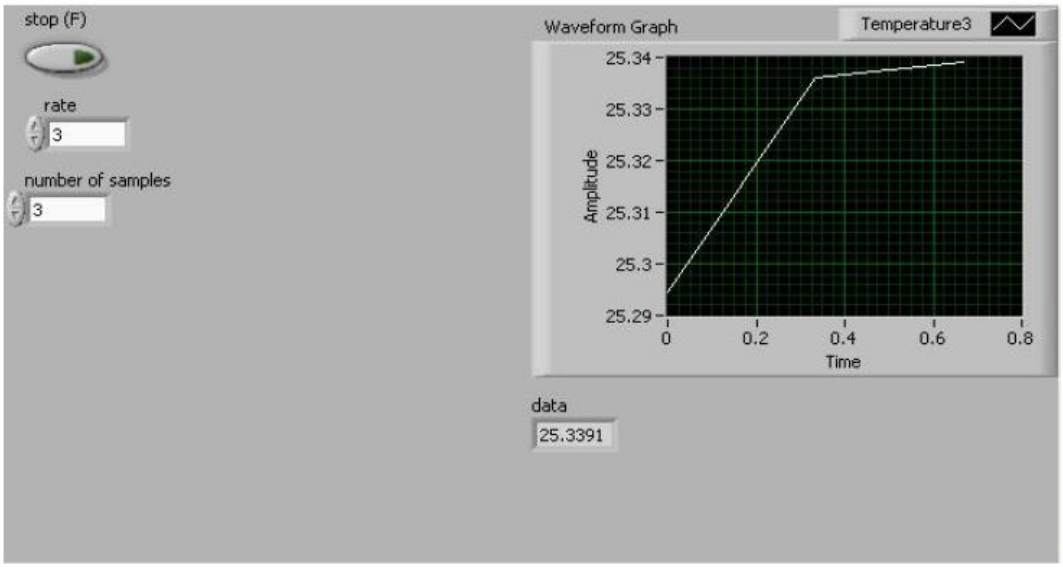

Figure 3.16: Front Panel for Data Acquisition

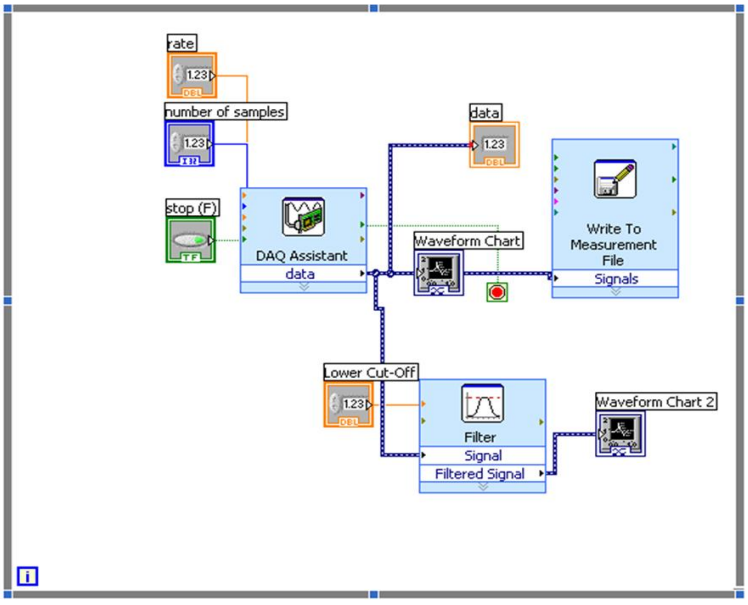

Figure 3.17: Block diagram of VI programmed using LabVIEW

3.5 Instrumentation

3.5.1 Radiometer

Global radiation of CH_4-O_2 flames were measured using a Mark IV series non contact temperature sensor & radiometer with 150° view angle and 0.1 to 92 µm wavelength ranges. The diameter of black circular surface is about 1 inch. Solar flux radiometer was also used, with a view angle of 180°and 0.1 to 20 µm wavelength ranges to measure CH_4-O_2 flame radiation. Figure 3.18 shows the Mark IV series radiometer.

Figure 3.18: Mark IV series radiometer

3.5.2 Temperature Controller

The CN7800 series controllers were used to control the required temperature of the steam line and burner (Figure 3.19). The CN7800 Series provides dual LED displays for local indication of process value and set point value. Control methods include on/off, PID, auto-tune and manual-tune. PID control is supported with 64 ramp/soak control actions. Two additional alarm outputs are standard on the CN7800 Series. The alarm outputs can be quickly configured by using the 13 built-in alarm functions. The controller communicates easily with the built-in RS485 interface.

Figure 3.19: Temperature Controller

3.5.3 VXM Stepping Motor Controller

VXM Stepping Motor Controller was used to move the traverse in horizontal and vertical direction for required experimental measurements (Figure 3.20). The VXM is a high performance, programmable, 2 phase, unipolar stepper motor controller.

Figure 3.20: VXM Stepping Motor Controller

3.6 Stoichiometric Calculations

The stoichiometric quantity of oxidizer is just that amount needed to completely burn a quantity of fuel. If more than a stoichiometric quantity of oxidizer is supplied, the mixture is said to be fuel lean; while supplying less than the stoichiometric oxidizer results in a fuel-rich or rich mixture. The stoichiometric oxidizer- (or air-) fuel ratio (mass) is determined by writing simple atom balances, assuming that the fuel reacts to form an ideal set of products. For a hydrocarbon fuel given by C_xH_y, the stoichiometricrelation can be expressed as:

$$C_xH_y + a\,(O_2 + 3.76N_2) \rightarrow xCO_2 + (y/2)\,H_2O + 3.76aN_2 \quad \text{(Air)}$$

$$C_xH_y + a\,(O_2 + bCO_2 + dH_2O) \rightarrow xCO_2 + (y/2)\,H_2O + dN_2 \quad \text{(Oxyfuel)}$$

The stoichiometric air-fuel ratio and oxygen to fuel ratio by mass can be found from:

$$\left[\frac{A}{F}\right]_{stoic} = \left[\frac{m_{air}}{m_{fuel}}\right]_{stoic} = \frac{4.76a}{1}\frac{MW_{air}}{MW_{fuel}}$$

$$\left[\frac{O}{F}\right]_{stoic} = \left[\frac{m_{Oxygen}}{m_{fuel}}\right]_{stoic}$$

Where MW_{air} and MW_{fuel} are the molecular weights of the air and fuel, respectively. The stoichiomteric values of CH_4 + air and CH_4+O_2 are shown in Table 3.1. The equivalence ratio was calculated using only the oxygen mass flow rate for oxyfuel combustion, as seen in the equation below:

$$\phi = \frac{O/F_{stoic}}{O/F_{actual}}$$

Table 3.1: Stoichiomteric value of CH_4 + air and CH_4+O_2

Fuel mixtures	Stoichiometric value
CH_4 + air	17.11
CH_4 + O_2	4

3.7 Estimation of Experimental Uncertainties

Random error was statistically determined based on the sample size and standard deviation of the data points. Bias error was found on the calibration error, typically 0.1- 1.5% of the full scale. The estimated uncertainties for flame stability at the bulk velocities, flame radiation, flame length and flame temperature are presented in Table 3.2.

Table 3.2: Estimated uncertainties as a percentage of the mean

Mean velocity (cm/s)	1.51%
Radiative Fraction (-)	2.78%
Flame Length (mm)	1.69%
Flame Temperature (K)	1.54%

Chapter 4: Results and Discussions

4.1 Flame structure and Flame Shape

Flame structure from the exit of a tubular burner depended on oxygen supply as shown in figure 4.1(a) and 4.1(b). On the left, a yellow sooty diffusion flame is shown which has no premixed oxygen. The flames become more lean as the oxygen concentration is increased to the highest concentration on the right side of figure 4.1. A lean fully oxygen premixed flame produced low soot concentrations and molecular radicals, CH and C_2 giving the flame the distinctive blue premixed color.

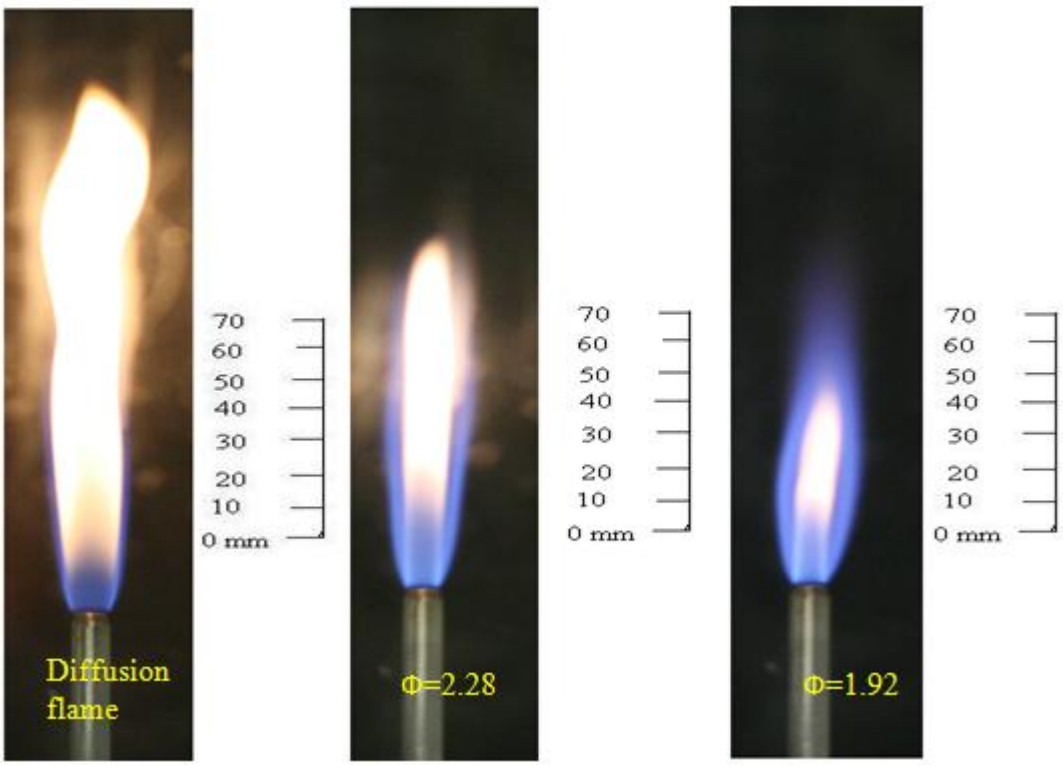

Figure 4.1(a): Different flame type of a 3 mm tubular burner on oxygen supply.

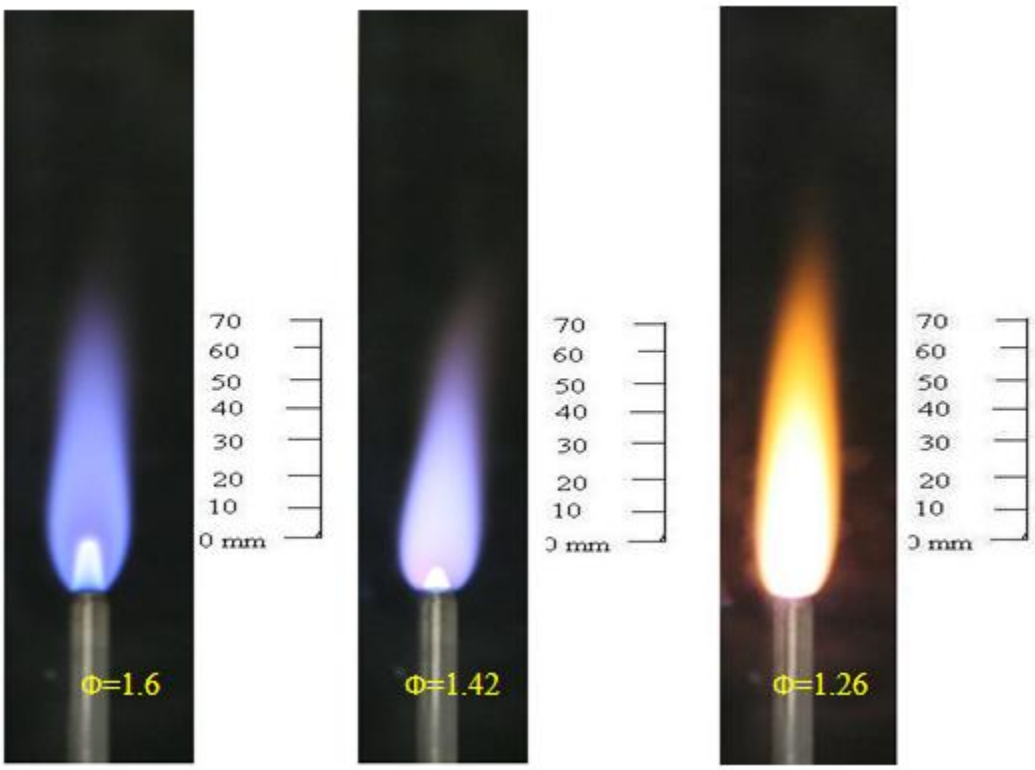

Figure 4.1(b): Different flame type of a 3 mm tubular burner on oxygen supply.

The CH_4-O_2 and 75%CH_4-25%CO_2-O_2 flames are shown in figure 4.2 and 4.3 at an equivalence ratio of 2. Both figures show that inner flame cone is surrounded by a longer less luminous outer reaction zone. The inner flame cone of CH4-O_2 flame is more luminous, but shorter in length compared to the 75%CH_4-25%CO_2-O_2 flame. This is due the presence of CO_2 diluents. The CO_2 diluents make the flame optically thin compared to the CH_4-O_2 flame and increase the inner flame cone length higher than CH_4-O_2 flame due to the higher bulk velocity. Therefore, the CH_4-O_2 flames are optically thicker than the 75%CH_4-25%CO_2-O_2 flames. A scaling is used in these images to measure the relative comparison of size between the different flames. The flame length is measured from the secondary or outer cone of the flame.

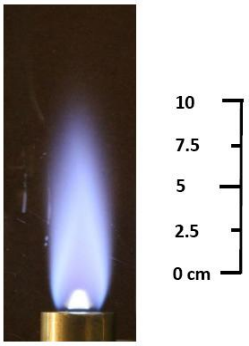

Figure 4.2: The flame of CH_4-O_2 using 6 mm burner at equivalence ratios of 2.

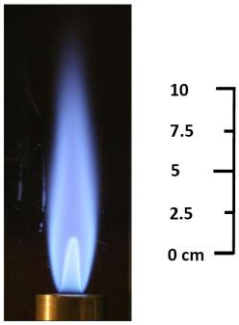

Figure 4.3: The flame of 75%CH_4-25%CO_2-O_2 using 6 mm burner at equivalence ratios of 2.

4.2 Effects of firing input and oxygen concentration on flame length

Figure 4.4 shows flame length versus the percentage of oxygen in the fuel-oxidizer mixture[1] at two different firing inputs. It can be seen from the figure that the flame length depends on both the fuel firing input and percentage of O_2 in the mixture. The flame length decreases from 270mm to 240mm and 240mm to 220mm as O_2 concentration increased for the 925W and 1313W firing inputs, respectively. Additionally, for a given percentage of oxygen, the flame length from fuel firing input 1313 W has higher length compared to a flame with a fuel firing input of 925 W. Fuel from 925 W is burned quickly compared to fuel from 1313 W for a given percentage of oxygen. Therefore, excess fuel from 1313 W is burned from atmospheric air that is called diffusion flame. For this reason, the flame length from fuel firing input 1313 W has higher length compared to a flame with a fuel firing input of 925 W.

[1] Percentage of oxygen in the fuel-oxidizer mixture=(Mass flow rate of oxygen/(Mass flow rate of oxygen+ Mass flow rate of fuel+ Mass flow rate of CO_2))*100

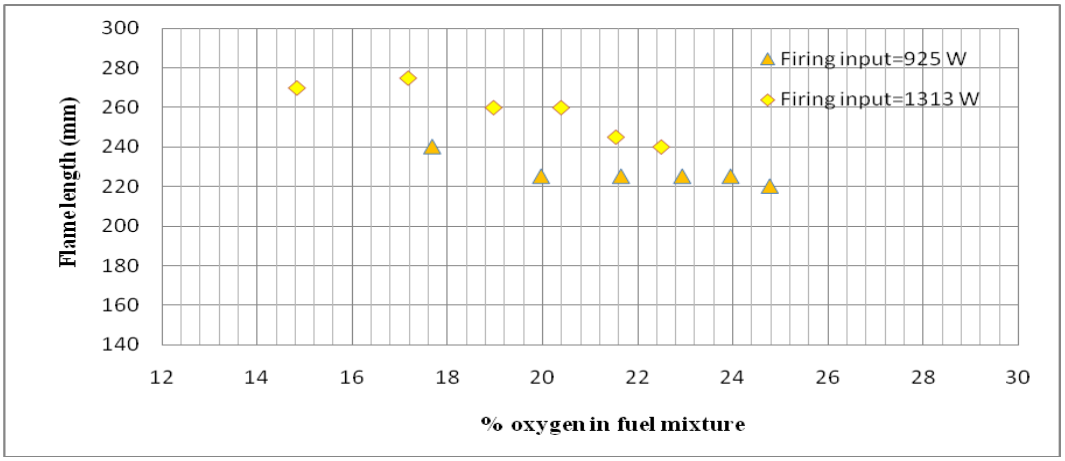

Figure 4.4: Flame length comparison between two firing inputs at CH_4-40%O_2-60% CO_2 composition using 6 mm diameter burner.

At varying different oxidizer compositions and constant firing input, the flame length was measured using 6 mm diameter tubular burner. Figure 4.5 shows the flame length versus bulk velocity for different O_2 and CO_2 concentrations in the fuel mixtures at constant fuel firing input (925 W). The percentage of O_2 in the oxidant mixture does not have a significant influence on the flame length for a given bulk velocity, however, the percentage of O_2 in the fuel-oxidizer mixture tends to correlate with an increase the flame length at higher bulk velocities.

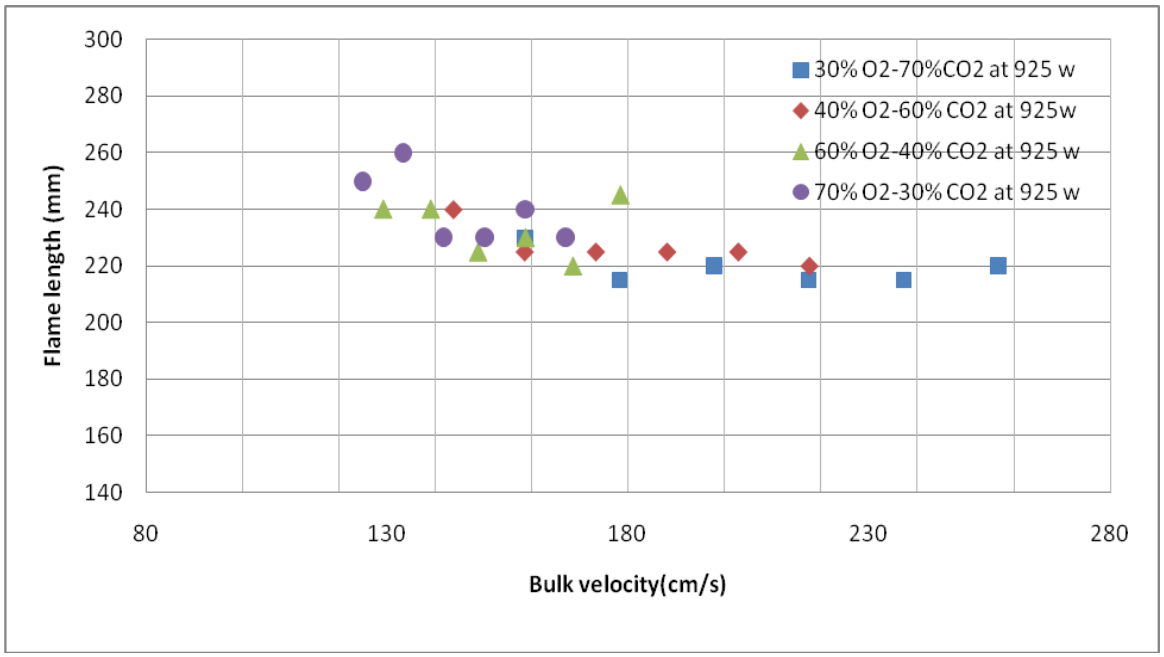

Figure 4.5: Flame lengths with varying different O_2 and CO_2 compositions at 925 W.

4.3 Stability of Flames

4.3.1 Stability of CH_4-Air and CH_4-O_2 Flames

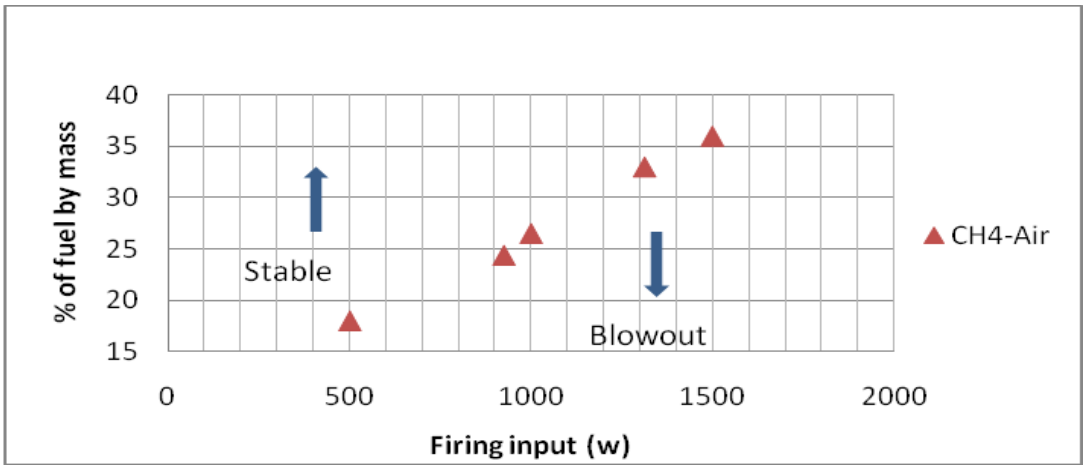

Figure 4.6: Stability map for CH_4-Air flame at different firing conditions using 3 mm diameter tubular burner.

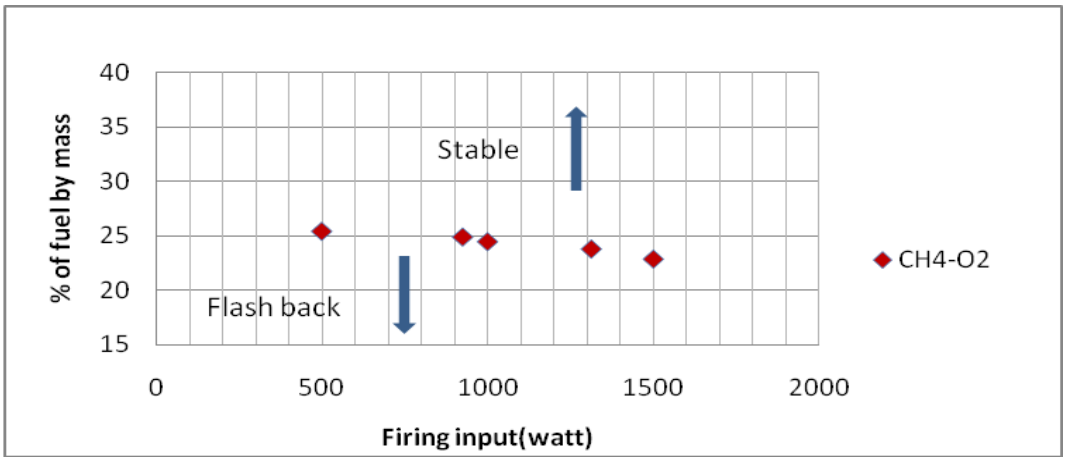

Figure 4.7: Stability map for CH_4-O_2 flame at different firing conditions using 3 mm diameter tubular burner.

The stability maps for CH_4-Air and CH_4-O_2 flames are shown in figures 4.6 and 4.7. At same operating conditions, the CH_4-air flame tends to blowout whereas CH_4-O_2 flame shows flashback behavior. Figure 4.8 shows that the adiabatic temperatures of CH4-O2 flames are higher than CH_4-air flames at any firing input conditions using Stanjan software. Since CH_4-O_2 has a higher flame temperature, the upstream gains more heat so that it preheats the unburned gases. Hence, the unburned gases enhance the flame propagation rate. The flame is more likely to flashback because the unburned gas temperature is increased. In case of CH_4-Air flame, flame tends to blow out due to higher bulk velocity than burning velocity

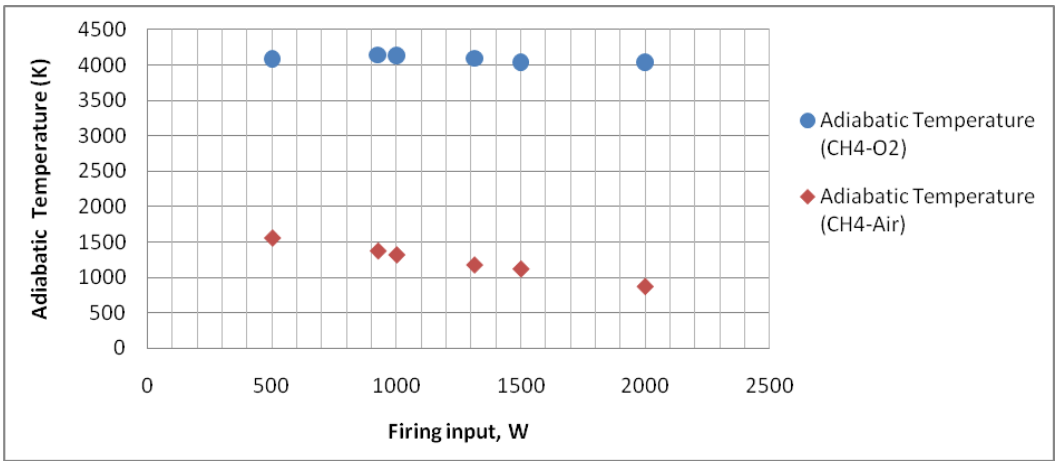

Figure 4.8: Adiabatic flame temperature of CH_4-O_2 and CH_4-Air at varying firing input.

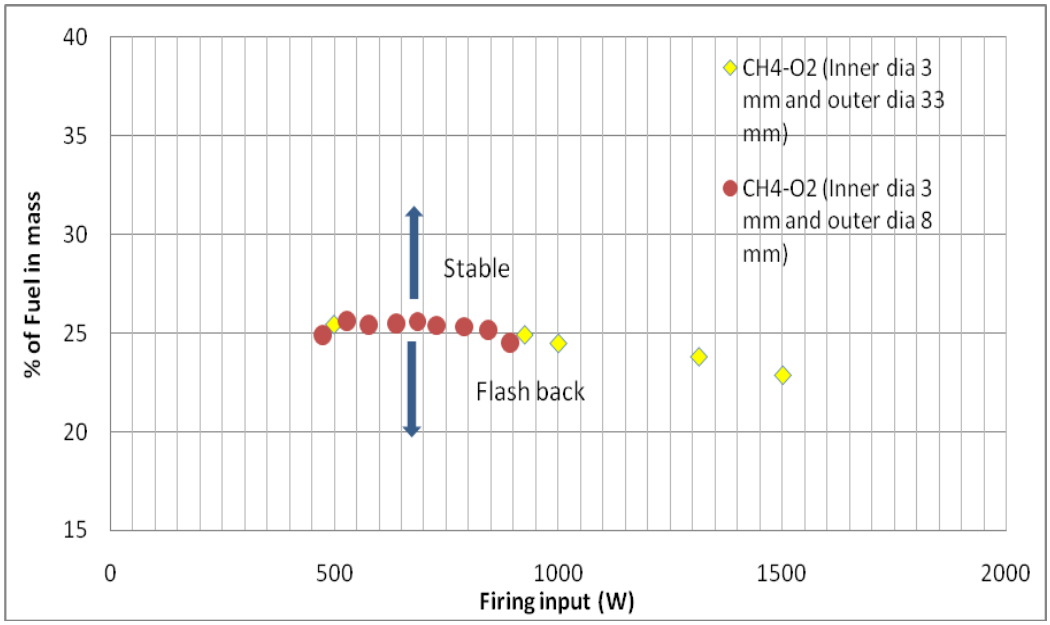

Figure 4.9: Stability map for CH_4-O_2 flame using 3 mm inner diameter with different outer diameter tubular burner at different firing conditions.

Figure 4.9 shows the comparison of stability maps of CH_4-O_2 flames using two different outer diameter burners with same inner diameter. It can be seen from the figure that there is no significant difference between the two different outer diameter burners with same inner diameter. Since outer

diameters are beyond the critical outer diameter. For this reason, heat dissipation rate from inner wall to outer wall is not affected by the different outer diameters.

4.3.2 Stability of CH_4-O_2 Flames using different diameters tubular burner (1mm-6mm)

Figures 4.10 thorough 4.16 present the stability results using different tubular burner diameters, ranging from 1 to 6 mm. The stability maps of CH_4-O_2 are plotted as the equivalence ratio versus bulk mass flow rate. The 1 mm diameter burner tube has exceptional flame operability characteristics compared to flames from larger diameter burner tubes for a given mass flow rate. The flame from the 1 mm diameter burner tube tends to extinguish rather than blowout or flash back, even though it is operated at lower mass flow rates, this is due to the quenching distance effect. Although at a higher temperature, the propagation rate of premixed laminar flames is retarded due to the large volumetric heat loss. Therefore, resulting flame is extinguished, while passing through this 1 mm burner tube. The flames from the 2 to 6 mm diameter burner tubes tend to flashback rather than extinguish or blowout. The burning velocities from these flames are higher than the bulk velocity of fuel mixture composition, therefore, the resulting flame in flashback. Hence larger diameter burners tend to more flash back than lower diameter of burners due to burning velocity. For these reason, the stability regime is increased as the burner diameter is decreased at a given mass flow rate.

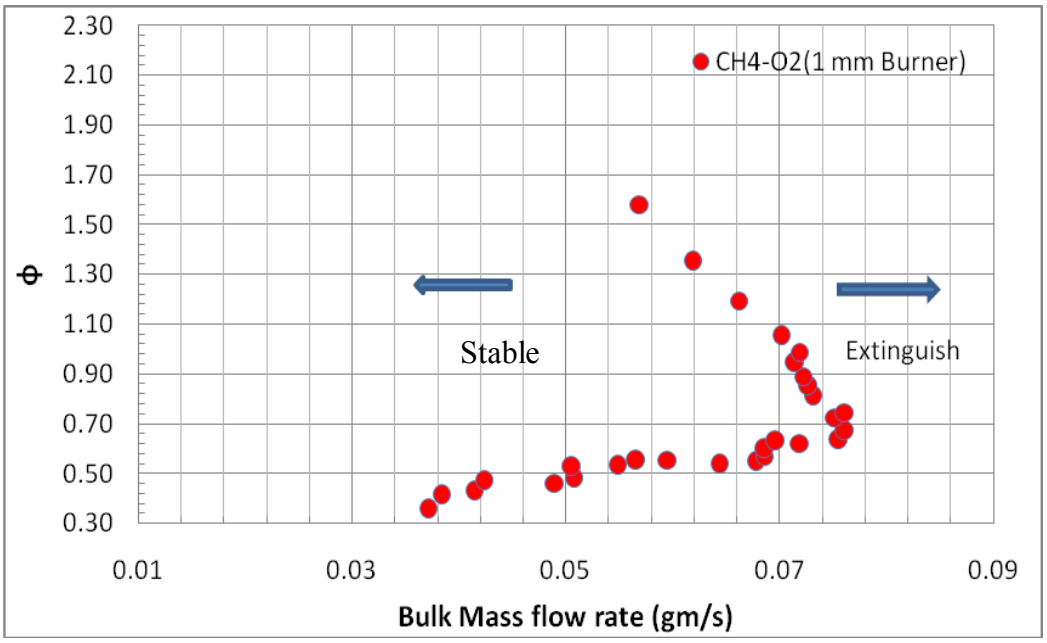

Figure 4.10: Stability map for CH_4-O_2 flame using 1 mm inner diameter tubular burner.

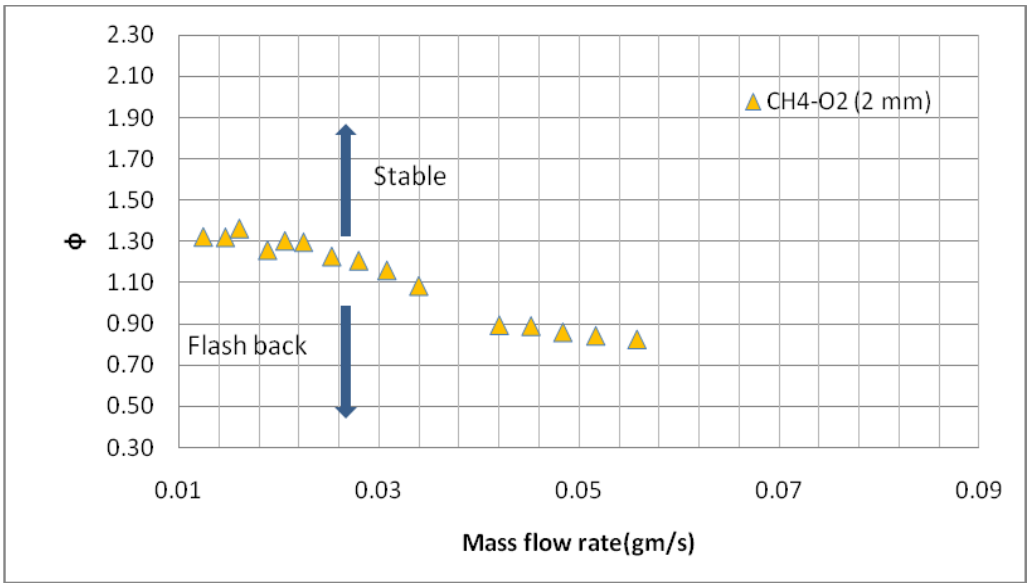

Figure 4.11: Stability map for CH_4-O_2 flame using 2 mm inner diameter tubular burner.

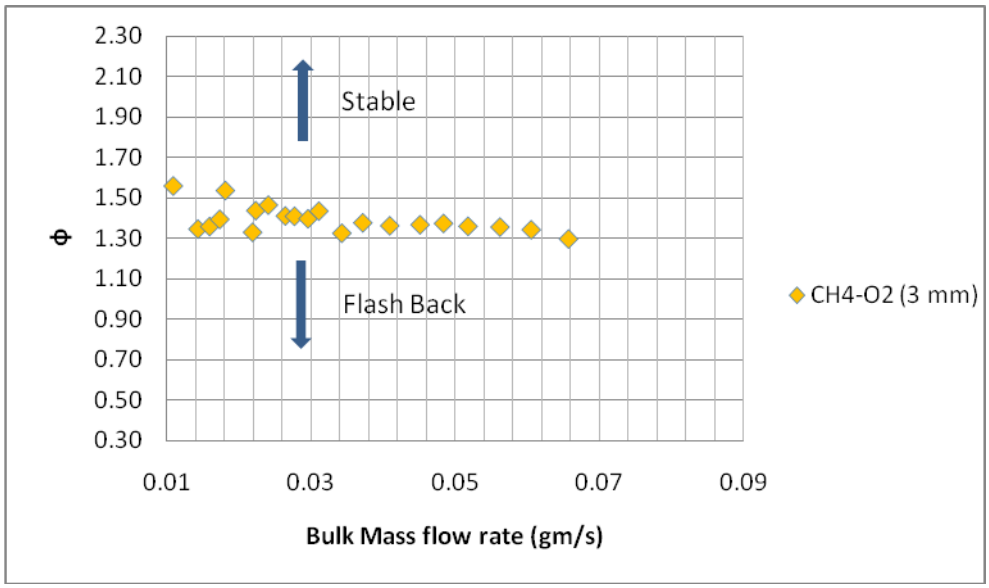

Figure 4.12: Stability map for CH_4-O_2 flame using 3 mm inner diameter tubular burner.

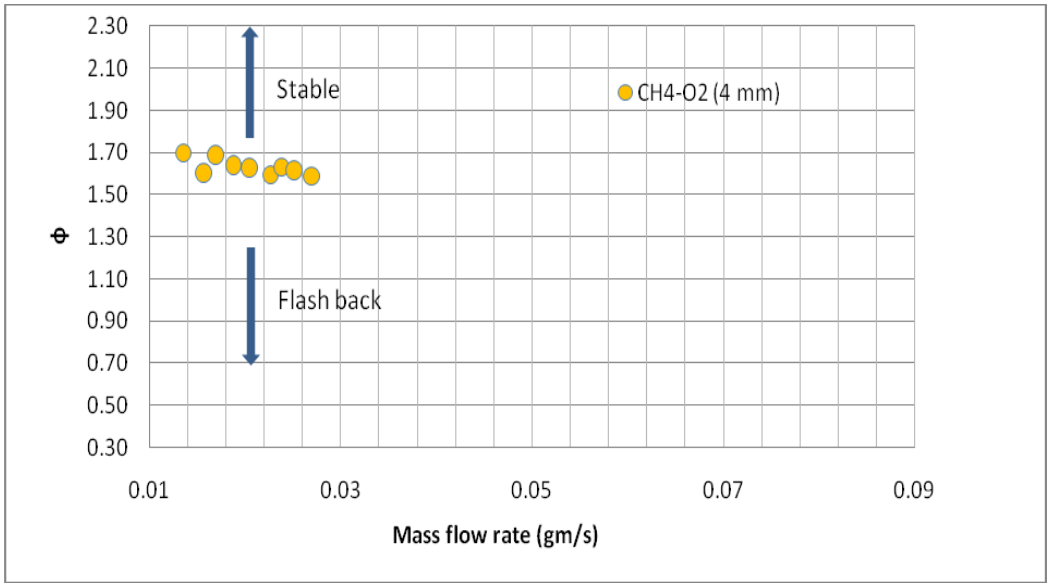

Figure 4.13: Stability map for CH_4-O_2 flame using 4 mm inner diameter tubular burner.

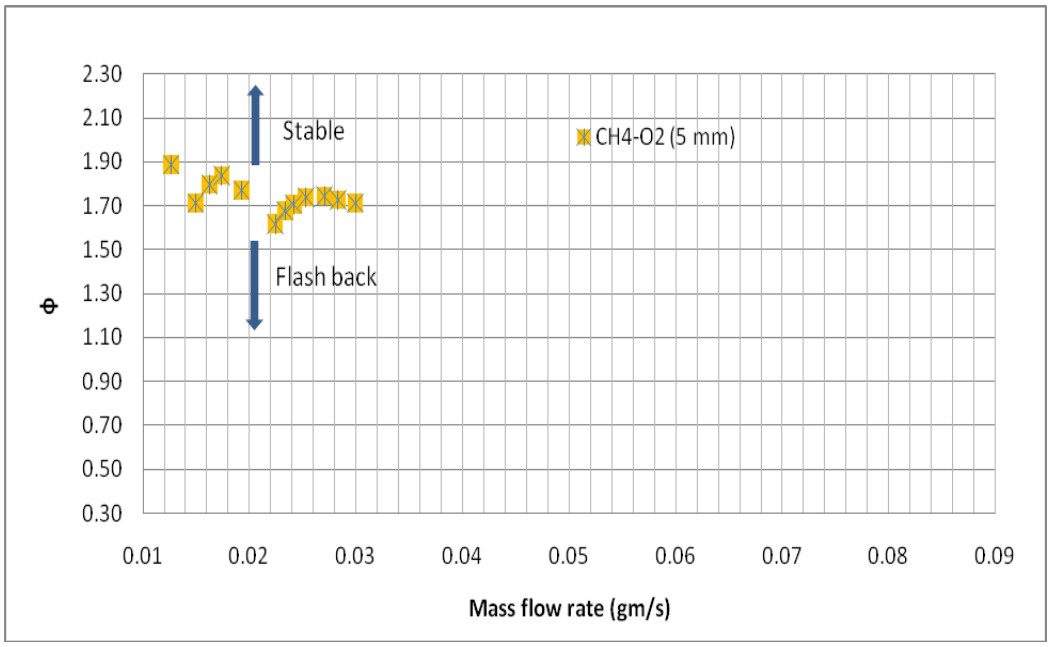

Figure 4.14: Stability map for CH_4-O_2 flame using 5 mm inner diameter tubular burner.

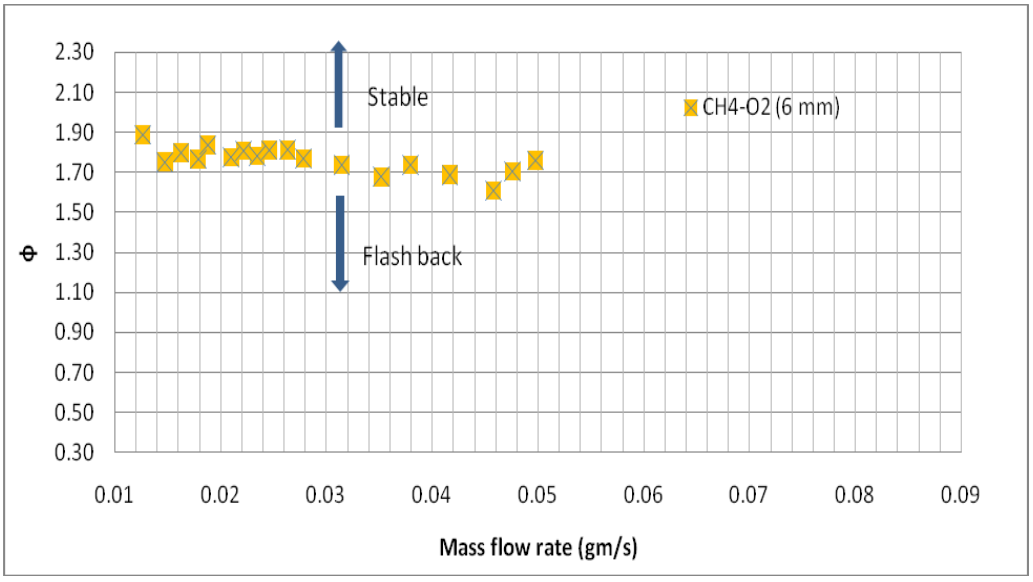

Figure 4.15: Stability map for CH_4-O_2 flame using 6 mm inner diameter tubular burner.

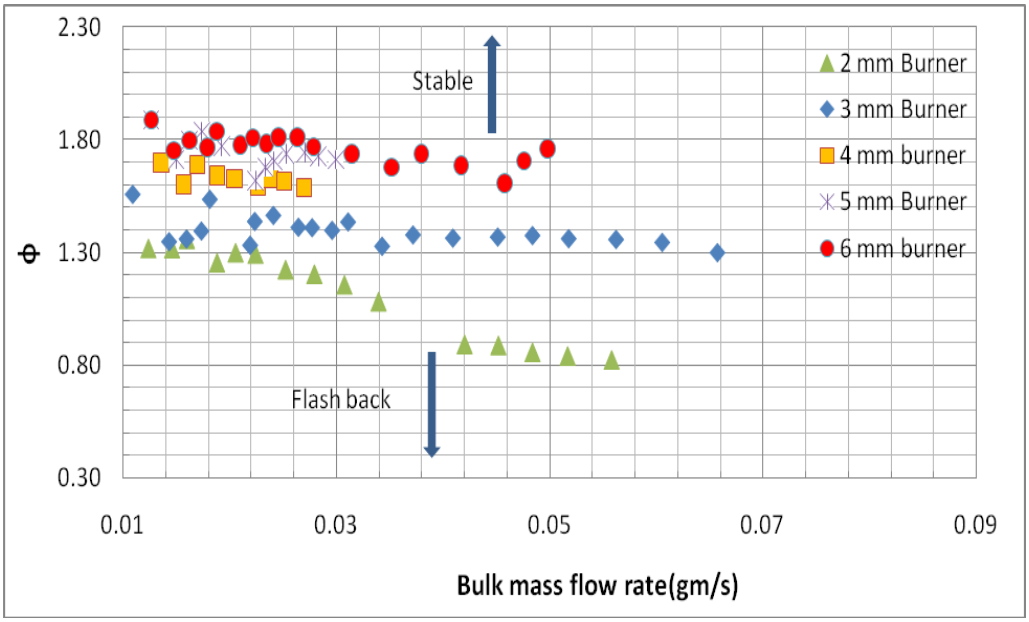

Figure 4.16: Stability map for CH_4-O_2 flame using varying diameter (2mm-6 mm) tubular burner.

4.3.3 Stability of CH_4-CO_2- O_2 flames

The stability map for CH_4-CO_2-O_2 flames is shown in Figure 4.16. Graph shows that the stability regime is increased with the concentration of CO_2 composition in the different fuel mixture. For a given mass flow rate using 3 mm diameter tubular burner, it shows that higher percentage CO_2 are more stable than lower percentage of CO_2 in the fuel mixture. In this cases CO_2 in the fuel mixture acts as a diluents, therefore, the propagation rate of reactions is reduced and reduced flame temperature. The propagation rate of burned gases towards the unburned gas mixture decreased due to the reduced temperature (Combustion, Glassman). Therefore, the stability regime is increased, as increased CO_2 concentration.

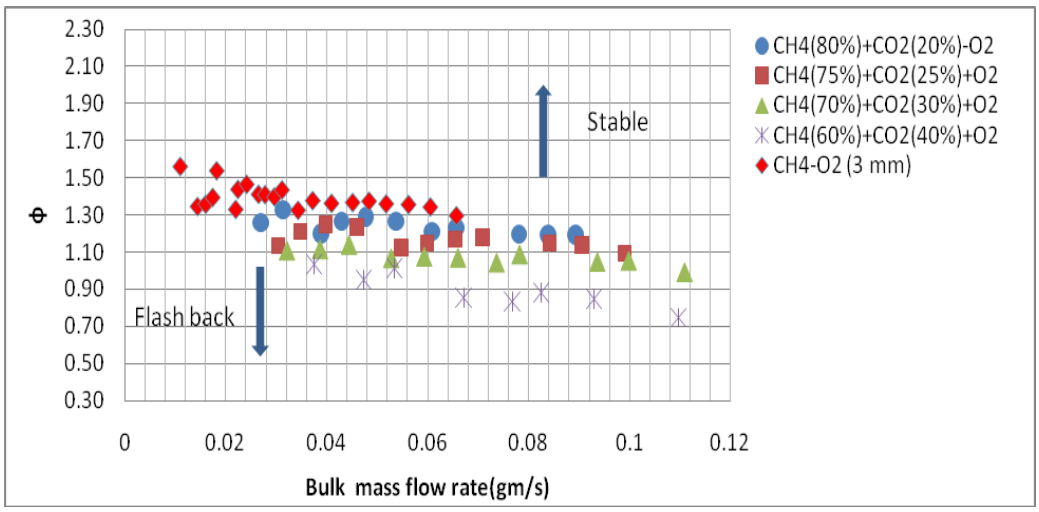

Figure 4.17: Stability map for CH_4-CO_2-O_2 flame using 3 mm diameter tubular burner.

4.3.4 Stability of CH_4-H_2O- O_2 flames

The stability map for CH_4-H_2O-O_2 flames is shown in Figures 4.18 and 4.19. For a given mass flow rate, the stability regime is increased with the concentration of H_2O composition in the different fuel mixtures using 9 mm diameter burner. In this cases H_2O in the fuel mixture acts as a diluents, therefore, unburned gas temperature is decreased and reduced the propagation rate of reactions. The propagation rate of burned gases towards the unburned gas mixture is decreased due to the reduced temperature (Combustion, Glassman). Since H_2O is added to oxygen to control the combustion temperature in oxy-fuel reactions

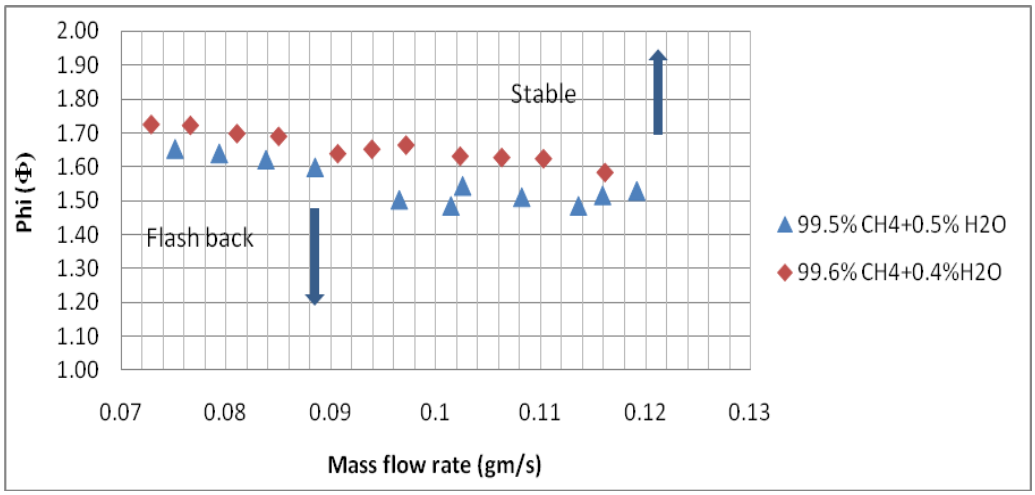

Figure 4.18: Stability map for CH_4-H_2O-O_2 (% of H_2O in fuel mixture) flame using 9 mm diameter tubular burner.

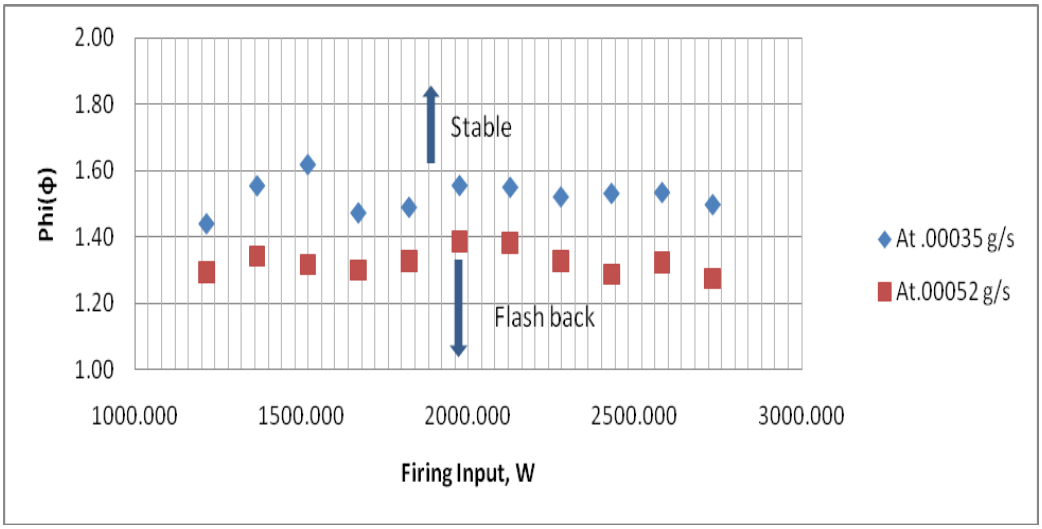

Figure 4.19: Stability map for CH_4-H_2O-O_2 flame using 9 mm diameter tubular burner.

4.3.5 Stability of CH_4-CO_2- H_2O- O_2 flames

The stability map for CH_4-CO_2- H_2O-O_2 flames is shown in Figure 4.20. For a given mass flow rate, the stability regime is increased with the concentration of CO_2-H_2O composition in the different fuel mixtures using 9 mm diameter burner. In this cases CO_2-H_2O in the fuel mixture acts as a diluents, therefore, the propagation rate of reactions is reduced and also reduced the flame temperature. The

propagation rate of burned gases towards the unburned gas mixture is decreased due to the reduced temperature. Figure 4.21 shows the comparison of stability map for CH_4-CO_2-H_2O-O_2 and CH_4-CO_2-O_2 flame. For a given mass flow rate, the stability regime of CH_4-CO_2-H_2O-O_2 flame is more increased than CH_4-CO_2-O_2 flame. Figure shows that H_2O (steam) has more diluents effect than CO_2 even though small percentage of H_2O in the fuel mixture.

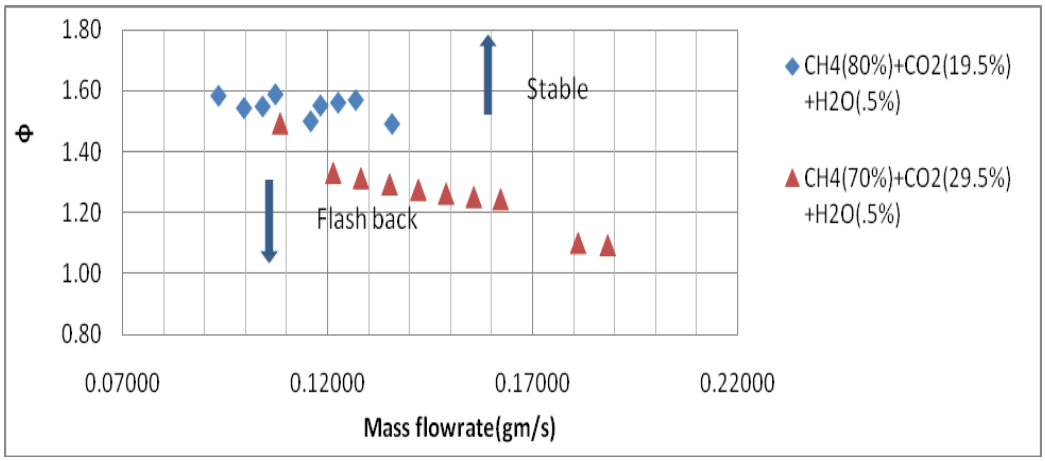

Figure 4.20: Stability map for CH_4-CO_2-H_2O-O_2 flame using 9 mm diameter tubular burner.

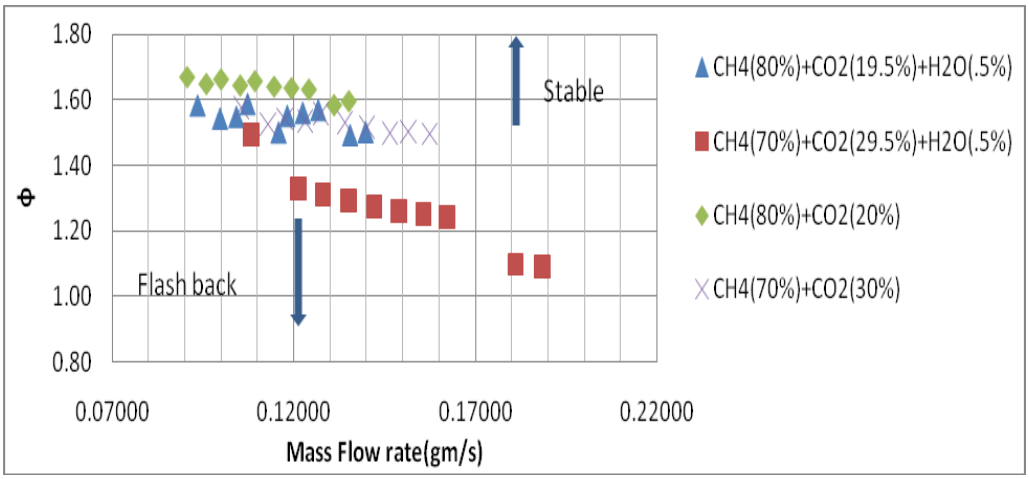

Figure 4.21: Comparison of stability map for CH_4-CO_2-H_2O-O_2 and CH_4-CO_2-O_2 flame using 9 mm diameter tubular burner.

4.4 Global Flame Radiation Measurements

At constant firing input with varying equivalence ratio, the radiative heat release rates are measured for both CH_4-Air and CH_4-O_2 flames using equation $F = \frac{q_r}{q_{in}}$, where q_r is the radiation output and q_{in} is the firing input to the combustion. The radiative heat release rate is plotted against equivalence ratio in figures 4.22. Figure shows that the radiative factor of CH_4-O_2 flames is higher than compared to CH_4-Air flames at same firing input conditions although CH_4-air flames did not stabilized at the lean conditions due to the presence of concentrated N_2 in the flue gas.

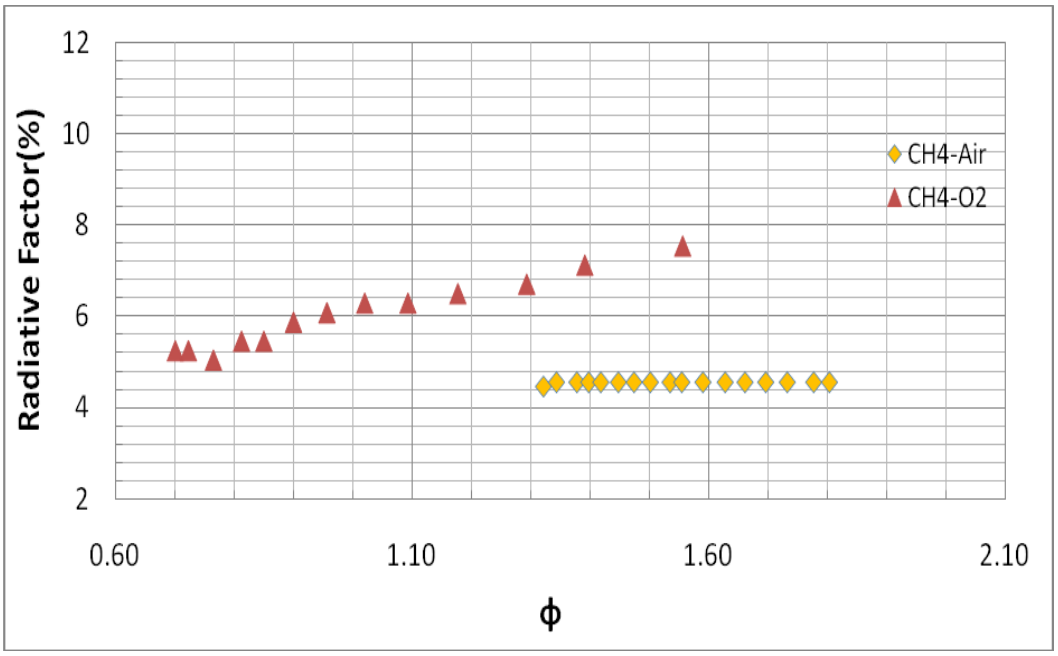

Figure 4.22: Comparison of radiative heat release rates between CH_4-Air and CH_4-O_2 flames.

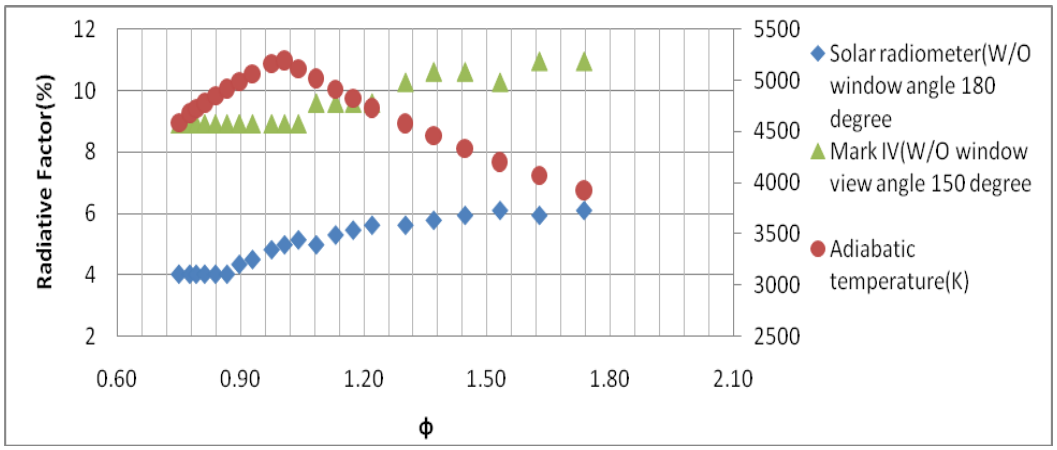

Figure 4.23: Radiation of CH_4-O_2 flames at constant firing rate using different radiometers.

The radiative heat release factor plotted against equivalence ratio and adiabatic temperature is shown in figure 4.23. The radiation of CH_4-O_2 flame is measured for varying equivalence ratios ranging from ϕ=0.75 to 1.73 using Solar radiometer and Mark IV series radiometer. Figure shows that the radiative heat release factor is almost constant for the lean flames in both radiometers whereas it increases more fuel rich conditions even though lower adiabatic flame temperature. The magnitude of radiative heat release factor using Mark IV series radiometer is higher than the solar radiometer measurements. This is due to the coverage of wide band wavelength ranges of mark IV series radiometer. Even though the adiabatic flame temperature was lower at the rich condition, the overall radiation measurement is increased due to an excess amount of unburned hydrocarbons and CH_4.

The radiative factor is plotted against percentage of CO_2 in the oxidant composition shown in figure 4.24. This was due to the presence of excess CO_2 in the oxidant, since CO_2 acts as strong radiation heat absorber and emitter.

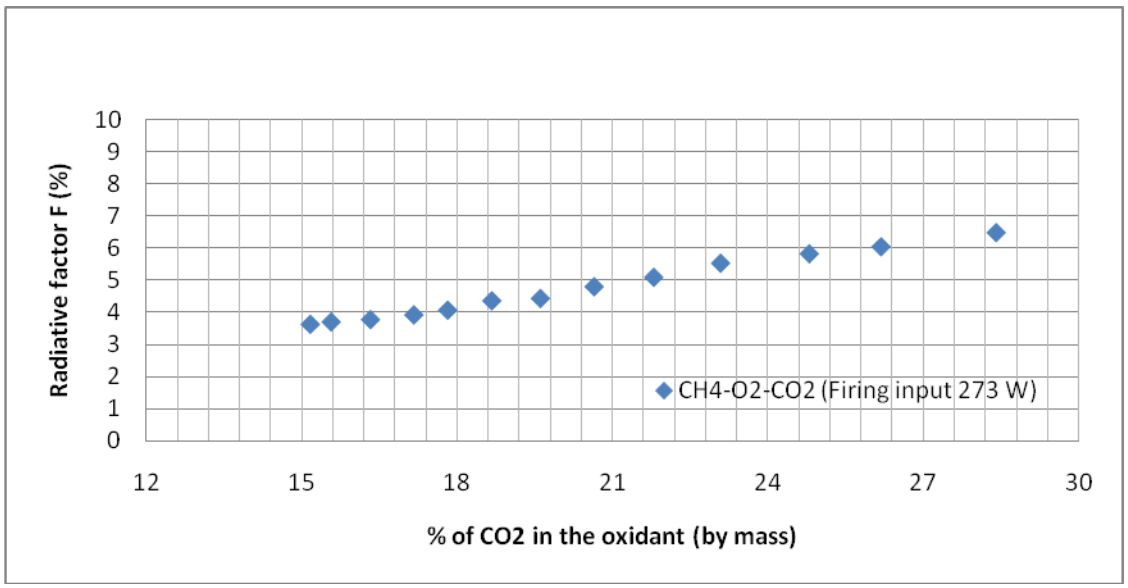

Figure 4.24: Radiation of heat release rates of CH_4-O_2 flames varying percentage of CO_2 in the oxidant.

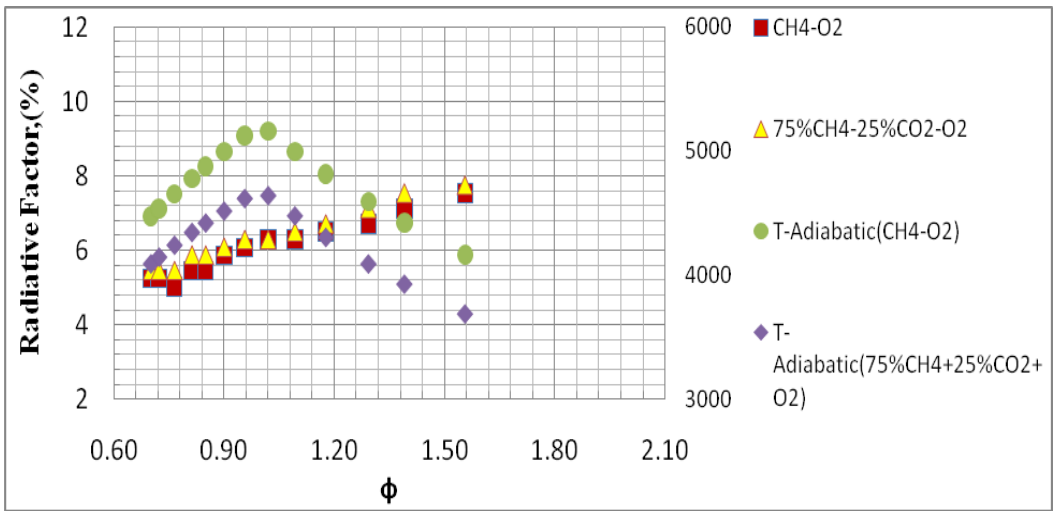

Figure 4.25: Radiation of CH_4-O_2 and CH_4-CO2-O2 flames at constant firing rate.

The radiative heat release factor of 75%CH_4-25%CO_2-O_2 and CH_4-O_2 flames plotted against equivalence ratio and adiabatic temperature is shown in figure 4.24. At constant firing input, the radiative heat release rates of 75%CH_4-25%CO_2-O_2 and CH_4-O_2 flames are more or less same. In

75%CH_4-25%CO_2-O_2 mixture, the CO_2 acts as diluents in the fuel mixture that reduces the flame temperature. Hence reduced flame temperature, the radiative heat release rates are also reduced. Even though the amount of radiation heat transfer is reduced due to the lower temperature, the reduced amount of radiation heat transfer is balanced by the presence of excess CO_2 in the fuel mixture. Since CO_2 acts as a strong radiation source for both emitting and absorbing perspective.

4.5 Flame Temperature

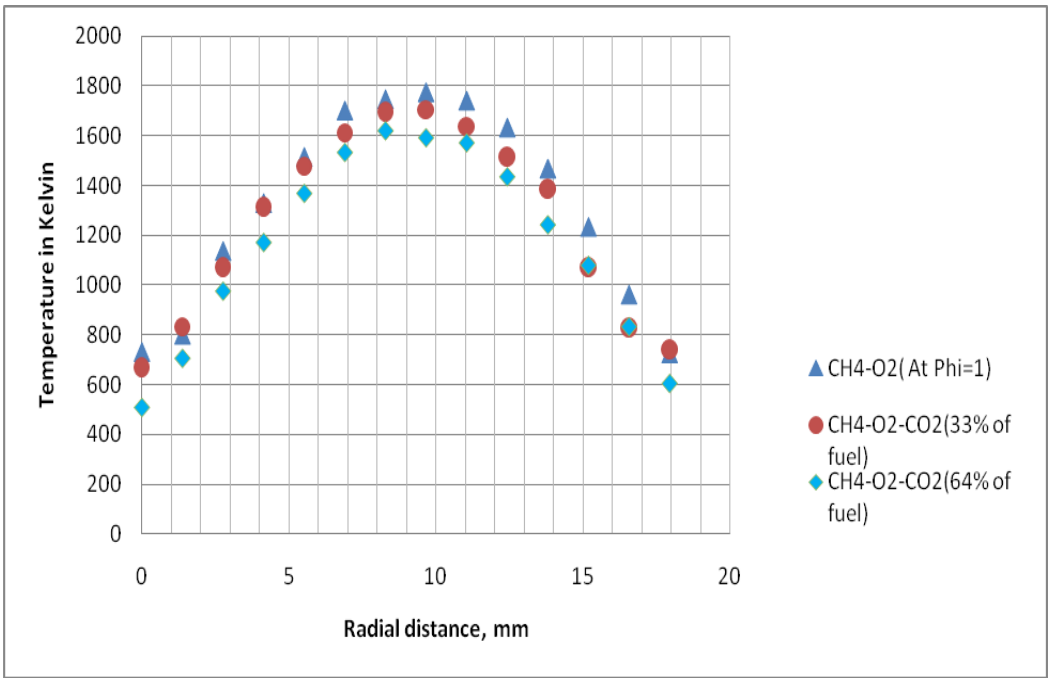

Figure 4.26: Flame temperature of CH_4-O_2 and CH_4-O_2-CO_2.

Flame temperatures were measured above two-third of flame length by S- type thermocouple with and without recirculation of CO_2 at equivalence ratio Φ=1 using 2 mm tubular burner. Figure shows that temperature is reduced with the increase of percentage of CO_2. Since CO_2 acts as a diluents, for this reason temperature is reduced with the concentration of CO_2.

Chapter 5: Summary and Conclusions

5.1 Summary of results

The flame length, stability of flame, global flame radiation measurements, and flame temperature of oxy-fuel combustion were experimentally investigated for the influence of high flame temperature from CH_4-O_2 combustion. Different tubular burners ranging in diameter from 1 to 6 mm and 9 mm were used with the designed burner facility. From these results and discussions, it was observed that flame lengths of oxy-fuel flames mainly depended on fuel firing input and affected, although less, the O_2 concentration in the fuel-oxidizer mixture. The flame length increased when the percentage of O_2 in the fuel-oxidizer mixture decreased. In addition, the flame length from the fuel firing input of 1313 W was significantly longer than flames from the firing input of 925 W. At the same operating conditions, it was observed that CH_4-Air flame tended to blowout, whereas CH_4-O_2 tended to flash back. Additionally, it was observed that oxy-fuel flames were prone to flash back due to the higher flame temperature. However, at a burner diameter of 1 mm the flame tended to extinguish. The stability regime for other burners, ranging from 2 to 6 mm, was also presented. Results showed that as the burner diameter decreased, flame stability increased. The addition of diluents CO_2 and H_2O in the feed stream shifted the stability regime from a fuel rich condition to near stoichiometric. The flame temperature also reduced with the concentration of CO_2. At constant firing input conditions, the radiative heat release rates of CH_4-O_2 flames were greater than CH_4-air flames. The radiative heat release factor was almost constant for the lean flames, whereas in rich conditions it increased as the equivalence ratio increased further. The radiative heat release rates also increased as the percentage of CO_2 was increased at a constant fuel firing input. The radiative heat release rates of 75%CH_4-25%CO2-O2 and CH_4-O2 flames were almost similar at constant firing input.

5.2 Conclusions

The following conclusions can be drawn from the current study presented in this thesis:

- Length of oxy-fuel is primarily affected by the fuel firing input and affected, although less, by the percentage of O_2 concentration.
- At the same operating conditions, the CH_4-Air flame tends to blow out, whereas CH_4-O_2 tends to flash back.
- As the burner diameter decreases, flame stability increases.
- Flame stability increases with the concentration of CO_2 and H_2O diluents.
- Radiative heat release rates of CH_4-O_2 are higher than CH_4-Air flames.
- At constant firing input conditions, radiative heat release rates of CH_4-O_2 flame are constant in lean flames, whereas it increases in rich condition.
- There is no significant difference between the radiative heat release rates of 75% CH_4-25% CO_2-O_2 and CH_4-O_2 flames at a constant firing input.
- As the concentration of CO_2 increases in the oxidizer, the flame temperature reduces.

5.3 Recommendations for future work

- The stability map can be measured with a recirculation ratio of CO_2 and H_2O at $\phi = 1$.
- Global radiation can be measured for CH_4-O_2-H_2O flame at constant firing input.

References

Amato A., Hudak B., D'Carlo P., Noble D., Scarborough D., Seitzman J. and Lieuwen T., 2011 "Methane Oxycombustion for Low CO_2 Cycles: Blowoff Measurements and Analysis" **Journal of Engineering for Gas Turbines and Power**, Vol. 133/061503-1

Andersson Klas, and Johnsson Filip 2007 "Flame and radiation characteristics of gas fired O_2/CO_2 combustion" **Fuel** 86 (2007) 656-668.

Andersson Klas, Johansson Robert, Hjartstam Stefan, Johnsson Filip, Leckner Bo 2008"Radiation intensity of lignied-fired oxy-fuel falmes" **Experimental Thermal and Fluid Science** 33 (2008) 67-76.

Andersson Klas, Normann Fredrik, Johnsson Filip, and Leckner Bo, 2008 "NO emission during Oxy-Fuel Combustion of Lignite" ***Ind. Eng. Chem. Res.*** 2008, 47, 1835-1845.

Buhre B.J.P., Elliot L.K., Sheng C.D., Gupta R.P., Wall T.F., 2005 "Oxy-Fuel combustion technology for coal-fired power generation" **Progress in Energy and Combustion Science** 31 (2005) 283-307.

Carbon sequestration Technologies Website, National Energy Technology Laboratory, **Department of Energy**, Web address: http://www.netl.doe.gov/technologies/carbon_seq/ 2007 Roadmap; Accessed June 16, 2011.

Croiset E., Thambimuthu K. V., 2001 "NO_x and SO_2 emission from O_2/CO_2 recycled coal combustion" **Fuel 80 (2001) 2117–2121**.

Croiset Eric, Thambimuthu Kelly, and Palmer Alan, 2000 "Coal combustion in O2/CO2 mixtures compared with air". **The Canadian Journal of Chemical Engineering**, Volume 78, April 2000.

Department of Energy (DOE), Innovations for existing plants/CO_2 emission control, oxy fuel combustion, National Energy Technology Laboratory, www.netl.doe.gov; Accessed July 25, 2011.

Ditaranto Mario, and Hals Jørgen, 2006 "Combustion instabilities in sudden expansion oxy–fuel flames" **Combustion and Flame** 146 (2006) 493- 512.

Hack Horst, Wheeler North America, USA, Shah Manish, Praxair Inc., USA. Presentation on oxy-fuel coal-fired combustion power plant system integration. March 5-6, 2008. **The third international oxy-combustion network meeting**.

Hjartstam Stefan, Andersson Klas, Johnsson Filip, Leckner Bo, 2009 "Combustion characteristics of lignite-fired oxy-fuel flames" **Fuel** 88 (2009) 2216-2224.

Hu Y.; Naito S.; Kobayashi N., 2000 "CO2, NOx and SO_2 emissions from the combustion of coal with high oxygen concentration gases" **Fuel** 79 (2000) 1925-1932.

Hu Y.Q., Kobayashi N., Hasatani M., 2001 "The reduction of recycled-NO_x in coal combustion with O_2 /recycled flue gas under low recycling ratio" **Fuel** 80 (2001) 1851-1855.

Huba Y.Q.; Kobayashi B.N.; Hasatania M., 2002 "Effects of coal properties on recycled NOx reduction in the coal combustion with O_2/recycled flue gas".

Jordal Kristin, Anheden Marie, Yan Jinying, Stromberg Lars., "2004 Oxyfuel combustion for coal-fired power generation with CO2 capture – opportunities and challenges". **Vattenfall Utveckling AB**, 162 87 Stockholm, Sweden, **Vattenfall AB**, 162 87 Stockholm, Sweden.

Kiga T., Takano S., Kimura N., Omata K., Okawa M., Mori T. and Kato M., 1997 " Characteristics of pulverized-coal combustion in the system of oxygen/recycled flue gas combustion" ***Energy Convers. Mgmt*** Vol. 38, Suppl., pp. S129-S134, 1997.

Kim Ho Keun, and Kim Yongmo, 2007 “Studies on Combustion Characteristics and Flame Length of Turbulent Oxy-Fuel Flames” **Energy and Fuels** 2007, 21, 1459-1467.

Kim Ho Keun; Kim Yongmo; Lee Sang Min; Ahn Kook Young, 2006 “NO reduction in .03-.02 MW oxy-fuel combustor using flue gas recirculation technology” **Proceedings of the Combustion Institute** 31 (2007) 3377-3384.

Kim, H. K.; Kim, Y, Lee, S.M.; Ahn, K.Y., 2006 “Emission characteristics of the 0.03 MW oxy-fuel combustor” **Energy Fuels** 2006, 20, 2125-2130.

Kimura N., Omata K., Kiga T., Takano S. and Shikisima S., 1995 “The characteristics of pulverized coal combustion in O_2/CO_2 mixures for CO_2 recovery” ***Energy Convers. Mgmt*** Vol. 36, no. 6-9, pp. 805-808, 1995.

Kroner, M., Fritz., J., and Sattelmayer, T. (2003), “Flashback Limits for Combustion Induced Vortex Brakdown in a Swirl Burner,” Journal of Engineering Gas Turbines and Power, Vol. 125, pp. 693-700.

LI Guo-neng, ZHOU Hao, and CEN Ke-fa, 2008 “Emission characteristics and combustion instabilities in an oxy-fuel swirl-stabilized combustor” **Journal of Zhejiang University SCIENCE A** 2008 9(11):1582-1589.

Liu H, Katagiri S, Kaneko U, Okazaki K., 2000 “Sulfation behaviour of limestone under high CO_2 concentration in O_2/CO_2 coal combustion” **Fuel** 79 (2000) 945–953.

Molburg JC, Doctor RD, Brockmeier NFSP., 2001 “ CO2 capture from PC boilers with O2-firing”. **Eighteenth annual international Pittsburgh coal conference, Newcastle, NSW, Australia**, December 4– 7, 2001.

Nozaki T., Takano S., and Kiga T., 1997 “Analysis of the flame formed during oxidation of pulverized coal by an O_2-CO_2 mixture” **Energy** Vol. 22, No. 2/3, pp. 199-205, 1997.

Ochs Thomas, Oryshchyn Danylo, Woodside Rigel, summers cathy, Patrick Brian, Gross Dietrich, Schoenfield Mark, Weber Thomas, and O'Brien Dan "Results of initial operation of the Jupiter Oxygen Corporation oxy-fuel 15 MWth burner test facility" **Energy Procedia** 1 (2009) 511-518.

Okazaki K., and Ando T., 1997 "NOx reduction mechanism in coal combustion with recycled CO_2" **Energy** Vol. 22 No. 2/3, pp 207-215, 1997.

Park Jeong, Park June Sung, Kim Hyun Pyo, Kim Jeong Soo, Kim Sung Cho, Choi Jong Geun, Cho Han Chang, Cho Kil Won, and Park Heung Soo, 2007 " NO Emission Behavior in Oxy-fuel Combustion Recirculated with Carbon Dioxide" **Energy and Fuels** 2007, 21, 121-129.

Sangras R, Chaˆtel-Pe´lage F, Pranda P, Farzan H, Vecci SJ, Lu Y,et al. Oxycombustion process in pulverized coal-fired boilers: a promising technology for CO2 capture. **The 29th international technical conference on coal utilization and fuel systems, Clearwater, Florida, April 18–22, 2004.**

Woycenko DM, van de Kamp WL, Roberts PA., 1995 "Combustion of pulverized coal in a mixture of oxygen and recycled flue gas", in summary of the **APG research program** (JOU2-CT92-0093, IFRF Doc F98/Y/4).

Appendix A

Sample Calculations

Stoichiometric Equations:

$$C_xH_y + a\,(O_2 + 3.76\,N_2) \rightarrow xCO_2 + (y/2)\,H_2O + (3.76a)\,N_2$$

$$where, a = x + \frac{y}{4}$$

$$\left[\frac{A}{F}\right]_{stoic} = \frac{a(32 + 3.76 * 28)}{12\,x + y}$$

For methane, (C_1H_4):

a = 1+4/4 = 2

AF_{stoic} = 2(32+ 105.28)/ (12+4) =17.16

Similarly,

OF_{stoic} = 2(32+0)/ (12+4) = 4

Equivalence Ratio:

$$\text{Equivalence Ratio, } \Phi = \frac{\left(\frac{A}{F}\right)_{stoic}}{\left(\frac{A}{F}\right)_{actual}}$$

Given AF_{actual} = 15.00

Then Φ = 17.16/15.00 =1.14

Given OF_{actual} = 3.95

Then Φ = 4/3.95 = 1.01

Estimated Uncertainties:

The overall uncertainty (ω) can be expressed mathematically as:

$$\omega = \sqrt{P2 + B2}$$

Where P is the random error and B is the bias error of the measurement. The random error was calculated from the following equation:

$$P = \frac{t_{\frac{\propto}{2}} S_x}{\sqrt{n}}$$

Where S_x is the standard deviation of the data points, n is the number of samples, and $t_{\frac{\propto}{2}}$ the student's t-distribution value for a 95% confidence interval.

Given measurements value; 1137.061, 1139.42, 1134.937, 1139.42, 1137.061, 1139.42, 1134.702, 1134.702, 1137.061, 1139.42

$\bar{X} = \frac{\sum X_i}{n}$ =1137.32;

$S_x = \sqrt{\frac{(X_i - \bar{X})^2}{n-1}}$ = 2.033819;

At 95% Confidence interval, α = 0.05 and α/2 = 0.025

$t_{\alpha/2}$ = 2.262;

$$Random\ error\ (P) = \frac{t_{\frac{\propto}{2}} S_s}{\sqrt{n}} = \frac{2.262 * 2.203819}{\sqrt{10}} = 1.45$$

If Bias error (B) = 1.5%, then overall error becomes;

$$\omega = \sqrt{(P^2 + B^2)} = \sqrt{[(1.45)^2 + (17.06)^2]} = 17.12;$$

Overall error in terms of %(ω) = (17.12/1137.32)100 = 1.51%

Steam calibration chart

Steam quality:

Pressure=40 psig

Temperature= 142^{o}C

Density= 2.05 kg/m^{3}

Metering valve (1 turn=25 divisions)

Water density= 1 gm/cm^{3}

Steam density= 0.00205 gm/cm^{3}

Fraction of turns (Metering valve)	Measured condensed water (gm/min)	Measured equivalent of steam (gm/min)	Measured equivalent of steam (mg/s)	Volumetric flow rates (LPM)
2/25	10.32	0.0211	0.35	0.010
5/25	15.11	0.0309	0.52	0.015
10/25	18.72	0.0383	0.64	0.019
15/25	21.63	0.0443	0.74	0.022
20/25	23.50	0.0481	0.80	0.024
25/25	25.09	0.0514	0.86	0.025

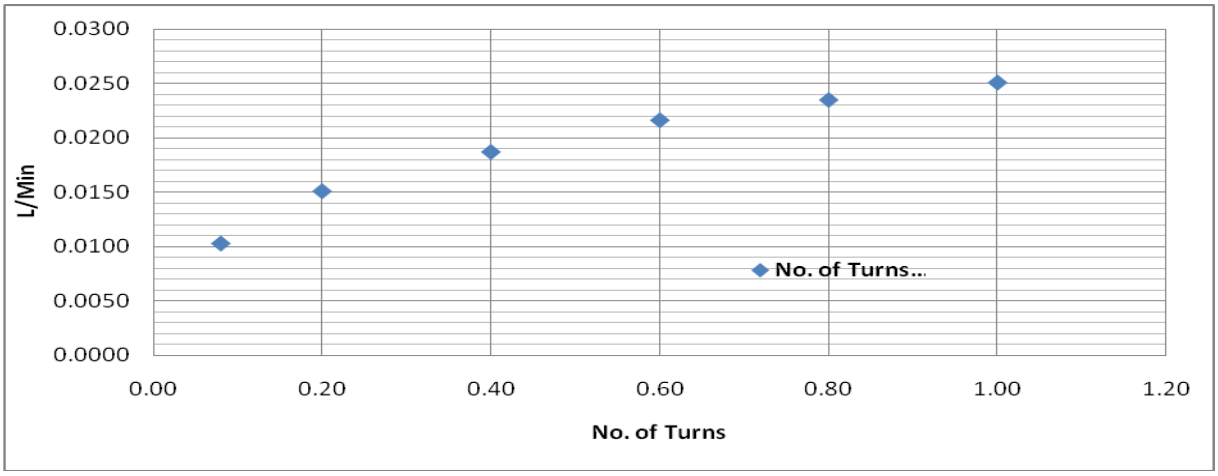

Appendix B

Nomenclature

Φ	=	Equivalence ratio
W	=	Watt
F	=	Radiative heat release factor
q_r	=	Radiation output
q_{in}	=	Firing input

Curriculum Vita

Md Rafiqul Islam was born on October 27, 1967. He received his Bachelor's of Science Degree in Electrical and Electronic Engineering from Khulna University of Engineering and Technology (KUET), Bangladesh in 1990. After graduation, he worked almost 12 years as an Assistant Engineer/Sub-Divisional Engineer under Bangladesh Power Development Board (BPDB). Ultimately, he completed his Master's of Science in Mechanical Engineering in 2011, focusing his research on the fundamental flame characteristics of oxy-fuel combustion at the Center for Space Exploration Technology Research (formerly Combustion and Propulsion Research Lab) under the guidance of Dr. Ahsan Choudhuri, Ph.D and Dr.Norman D. Love, Ph.D. His accomplishments include presenting and publishing one conference paper for ASME and one article for the Southwest Energy Science and Engineering Symposium. He was president of the Bangladesh Student Association (BSA) at UTEP (2010-2011), and a student member of the ASME.

Permanent address: 3500 Sun bowl Dr. Apt. 72
El Paso, TX 79902

This thesis is typed by Md Rafiqul Islam